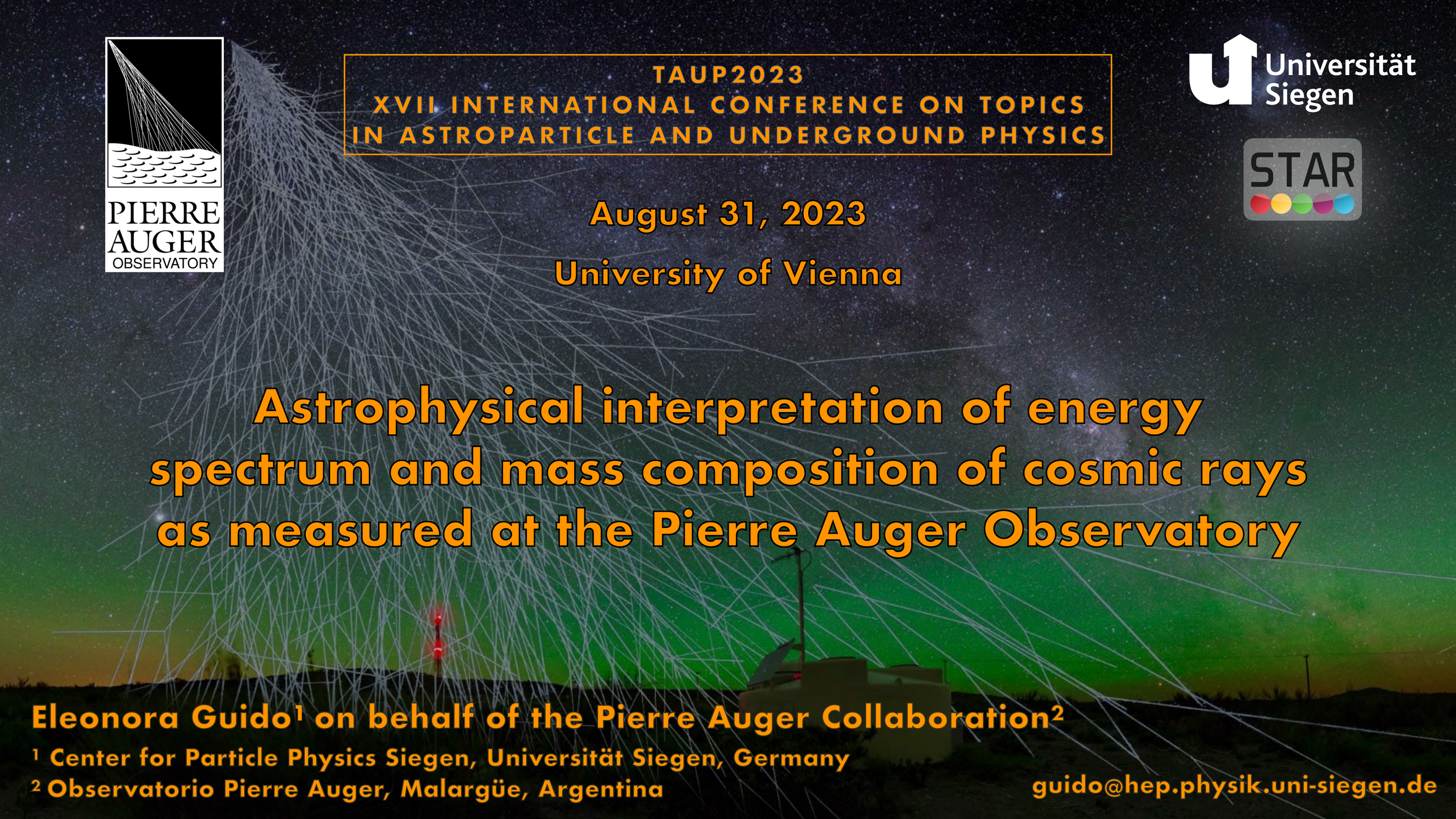

TAUP2023
XVII INTERNATIONAL CONFERENCE ON TOPICS
IN ASTROPARTICLE AND UNDERGROUND PHYSICS

August 31, 2023

University of Vienna

Astrophysical interpretation of energy spectrum and mass composition of cosmic rays as measured at the Pierre Auger Observatory

Eleonora Guido[1] on behalf of the Pierre Auger Collaboration[2]

[1] Center for Particle Physics Siegen, Universität Siegen, Germany

[2] Observatorio Pierre Auger, Malargüe, Argentina

guido@hep.physik.uni-siegen.de

Outline

- **The Pierre Auger Observatory** (brief introduction)
- **Measurements of the energy spectrum and mass composition** of ultra-high energy cosmic rays (UHECRs)

  → still open questions about their interpretation
- **Combined fit of the Pierre Auger Observatory measurements** (spectrum and composition) **across the ankle**

  Simple astrophysical model with different superposed components fitted to data

  Study of the effect of systematic uncertainties (from models and measurements)

  → constraints on the source properties [JCAP05(2023)024]
- **Preliminary analyses recently presented at the ICRC2023:**
  - constraints on source properties from **cosmogenic neutrino limits** [PoS(ICRC2023)1520]
  - investigation of the **extragalactic magnetic field impact** on the fit results [PoS(ICRC2023)288]
- **Conclusions and outlook**

The Pierre Auger Observatory

- **Largest observatory in the world for the detection of ultra-high-energy cosmic rays**

- Located in Argentina, close to Malargüe (~1400 m a.s.l.)
- **Ground-based experiment** detecting air-showers
- **Hybrid detection technique** (SD+FD)

~450 members from ~90 institutions in 17 countries

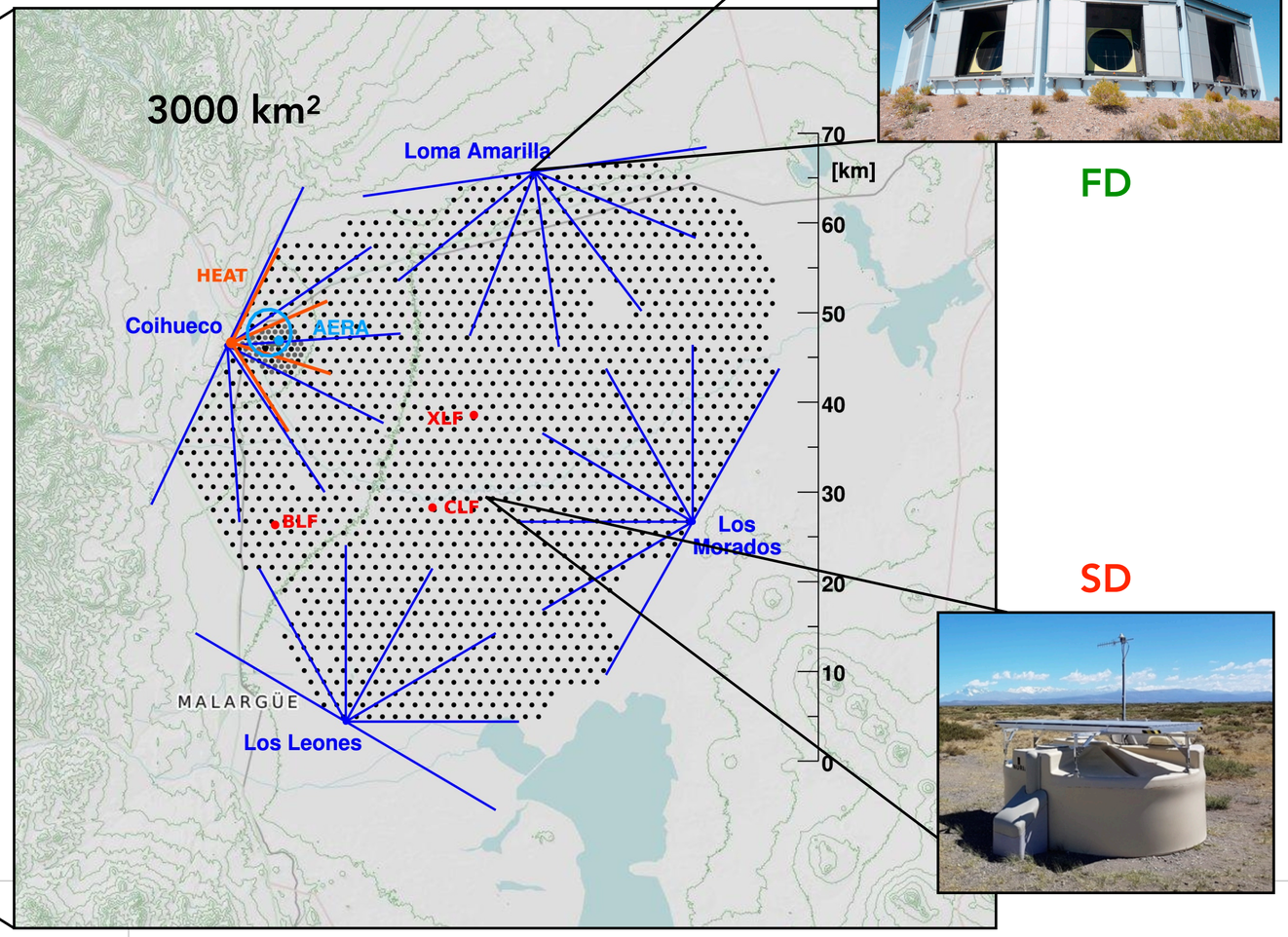

FD

SD

Energy spectrum and mass composition measurements

Energy spectrum for the events measured with the SD array

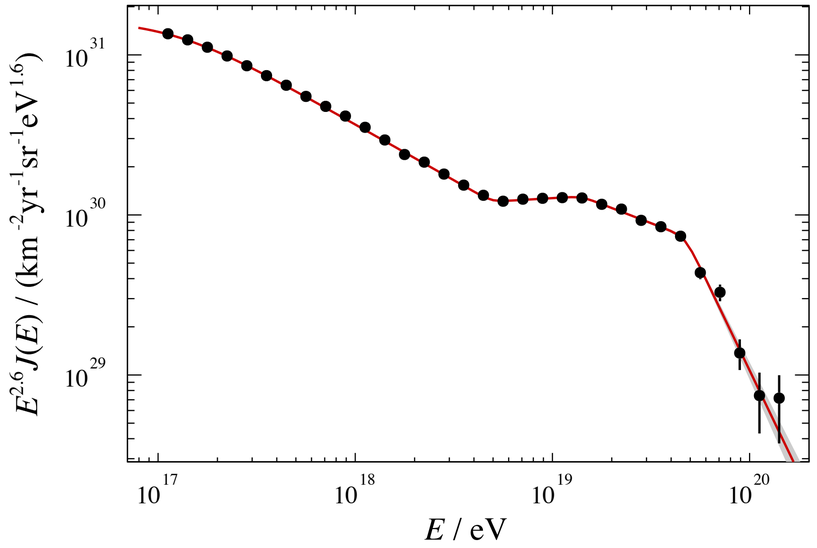

The X_{max} distribution in each energy bin is sensitive to the mass composition

→ first two moments shown for figurative purposes

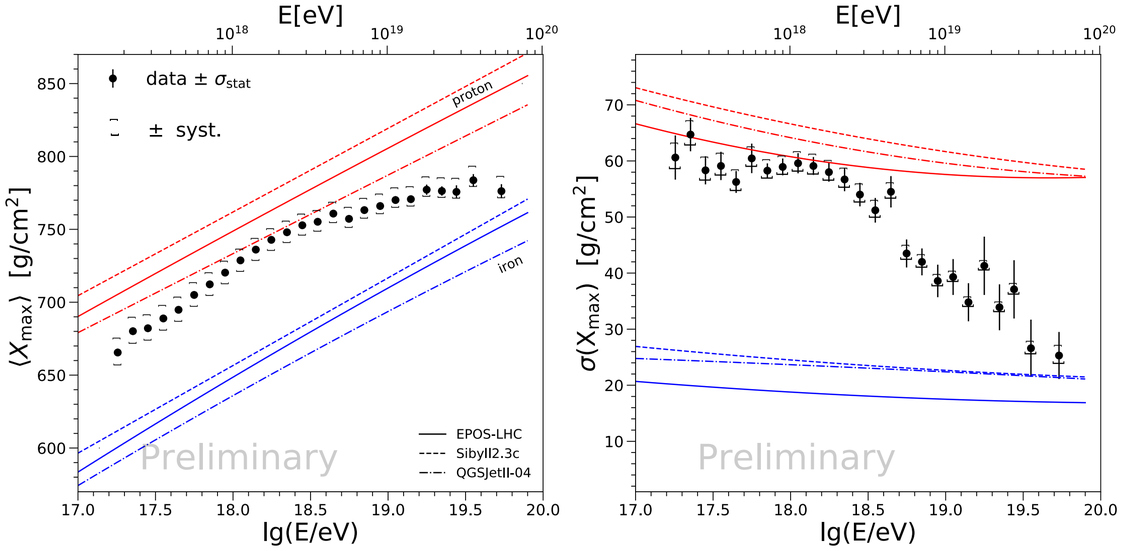

Data in $\log_{10}$(E/eV) bins of 0.1 width:

- Energy spectrum up to $10^{20.2}$ eV
- X_{max} distributions: up to $10^{19.7}$ eV (+ 1 additional bin for events above), binned in intervals of X_{max} of 20 g cm^{-2}

The Pierre Auger Collaboration, Eur. Phys. J. C 81, 966 (2021)
A.Yushkov for the Pierre Auger Collaboration PoS(ICRC2019)482

Energy spectrum and mass composition measurements

Energy spectrum for the events measured with the SD array

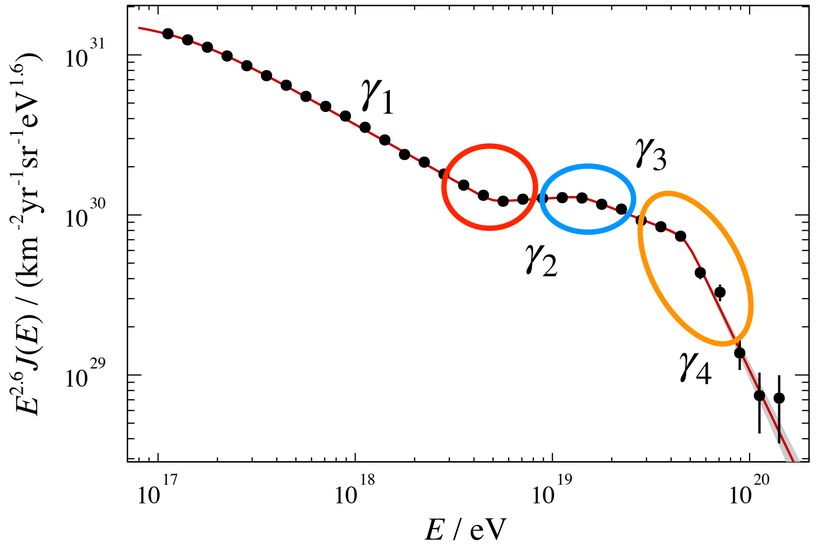

- **Hardening at ~6×10^{18} eV (ankle)**
- **Softening at ~1×10^{19} eV (instep)**
- **Suppression at ~5×10^{19} eV** → energy cut off

Propagation effect and/or maximum energy at the acceleration

The X_{max} distribution in each energy bin is sensitive to the mass composition

→ **first two moments shown for figurative purposes**

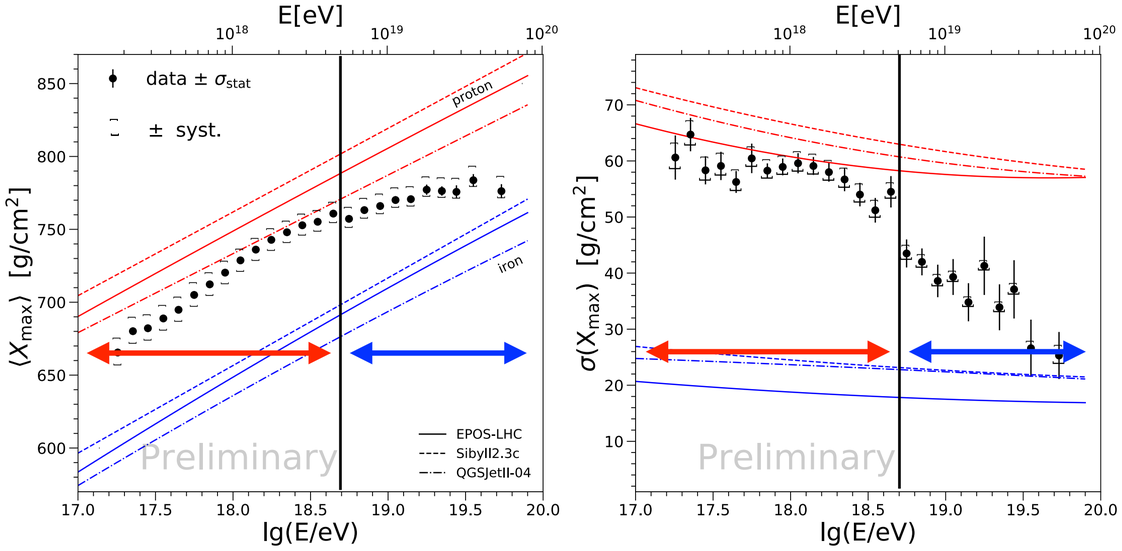

- **Below the ankle: mass composition gets increasingly lighter**
- **At the ankle: mixed composition**
- **Above the ankle: increasingly heavier and less mixed**

→ superposition of alternating and heavier groups of elements

→ increasingly sparse statistics up to ~10$^{19.7}$ eV

The Pierre Auger Collaboration, Eur. Phys. J. C 81, 966 (2021)
A.Yushkov for the Pierre Auger Collaboration PoS(ICRC2019)482

Energy spectrum and mass composition measurements

Energy spectrum for the events measured with the SD array

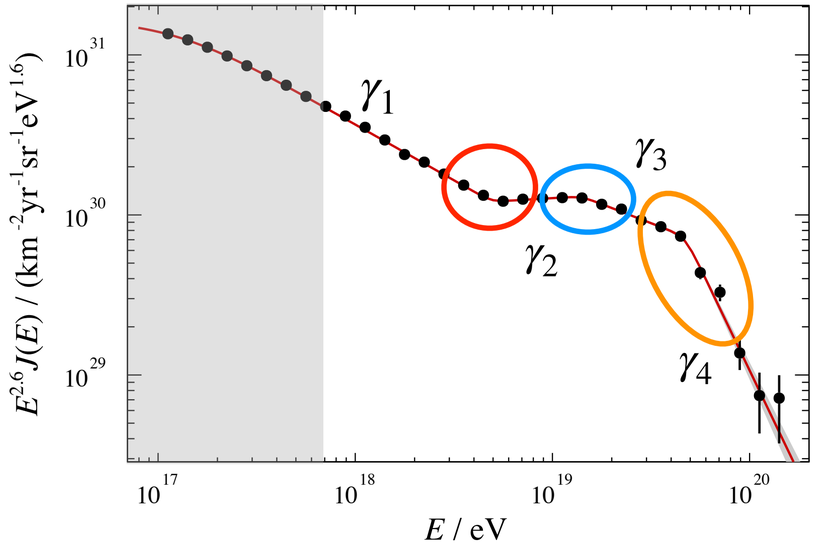

The X_{max} distribution in each energy bin is sensitive to the mass composition

→ first two moments shown for figurative purposes

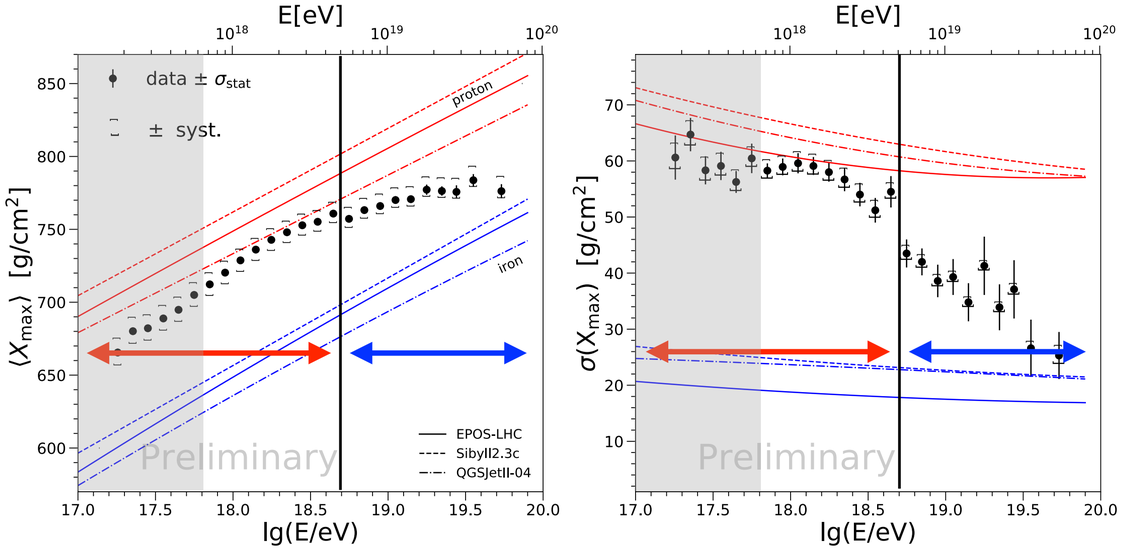

Combining the information from the two data sets is crucial to interpret the features

- We aim at including the ankle region
- We want to focus on the energy region where the Galactic CRs are not dominant anymore

} **Data above E ~ 6 x 10^{17} eV are considered**

The Pierre Auger Collaboration, Eur. Phys. J. C 81, 966 (2021)
A.Yushkov for the Pierre Auger Collaboration PoS(ICRC2019)482

The combined fit

CR$_S$ EJECTED BY EG ACCELERATORS

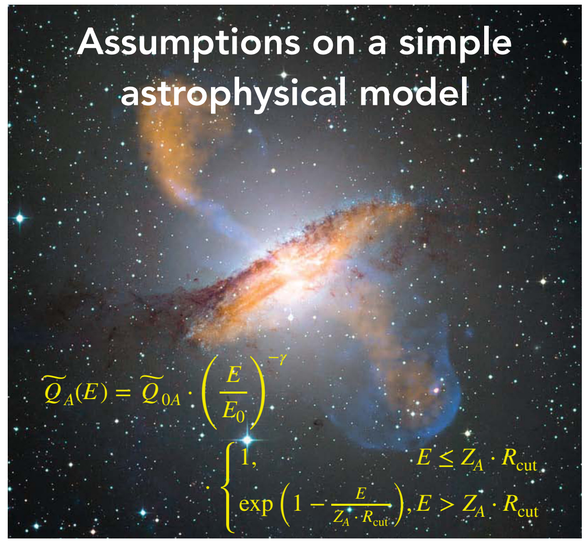

Generic populations of extragalactic sources:

- population of identical sources
- uniform distribution (except for a local overdensity for $d < 30$ Mpc)
- ejection of **n representative nuclear species A**, chosen among ^{1}H, ^{4}He, ^{14}N, ^{28}Si, ^{56}Fe

$$\widetilde{Q}_A(E) = \widetilde{Q}_{0A} \cdot \left(\frac{E}{E_0}\right)^{-\gamma} \cdot \begin{cases} 1, & E \le Z_A \cdot R_{\rm cut} \\ \exp\left(1 - \frac{E}{Z_A \cdot R_{\rm cut}}\right), & E > Z_A \cdot R_{\rm cut} \end{cases}$$

The combined fit

Choice of propagation models for uncertain quantities

CR$_S$ EJECTED BY EG ACCELERATORS

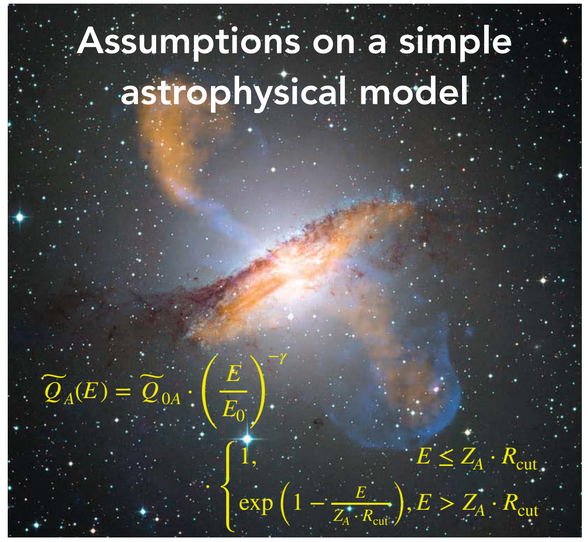

PROPAGATION THROUGH THE INTERGALACTIC MEDIUM

SIMPROP

Models are chosen for:

→ **photo-disintegration cross sections $\sigma_{\rm pd}$**

→ **EBL spectrum and evolution**

[1] R. Aloisio et al, JCAP 11 (2017) 009

The combined fit

CR$_S$ EJECTED BY EG ACCELERATORS

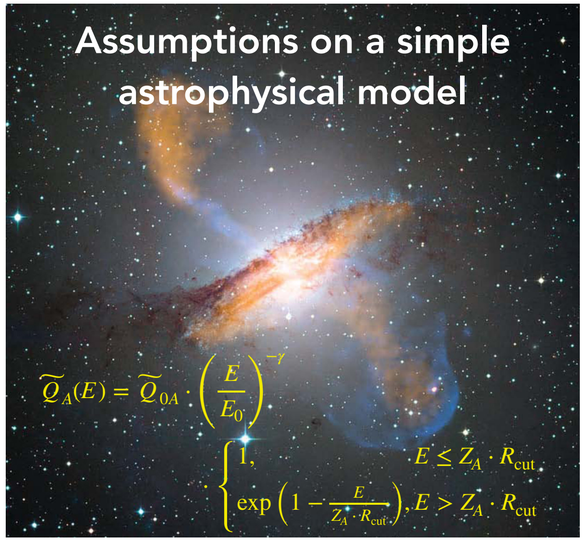

Choice of propagation models for uncertain quantities

PROPAGATION THROUGH THE INTERGALACTIC MEDIUM

SIMPROP

Choice of hadronic interaction model

PRODUCTION OF SHOWERS IN THE ATMOSPHERE

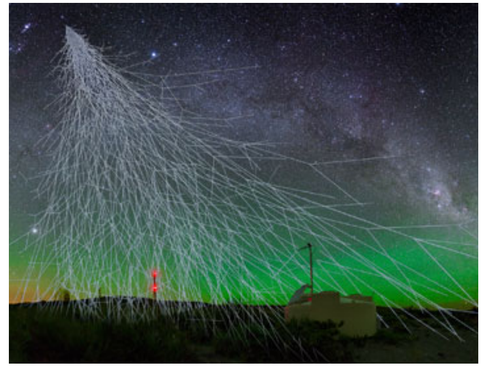

[1] R. Aloisio et al, JCAP 11 (2017) 009

The combined fit

CR$_S$ EJECTED BY EG ACCELERATORS

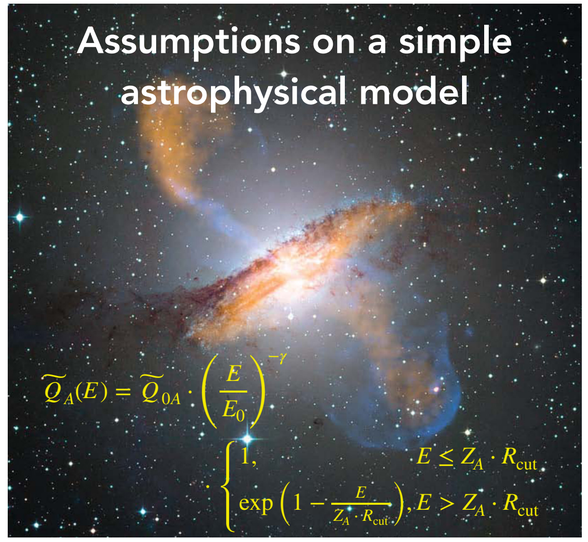

Choice of propagation models for uncertain quantities

PROPAGATION THROUGH THE INTERGALACTIC MEDIUM

SIMPROP

Choice of hadronic interaction model

PRODUCTION OF SHOWERS IN THE ATMOSPHERE

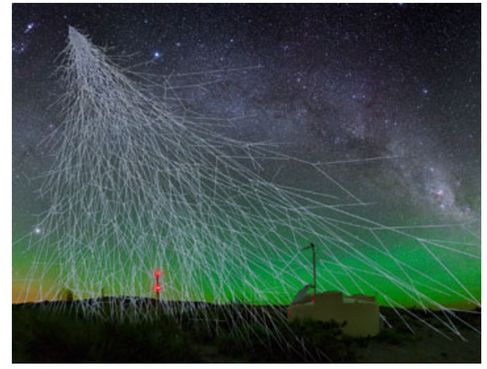

Detector effects are included

COMPARISON WITH THE OBSERVED DATA

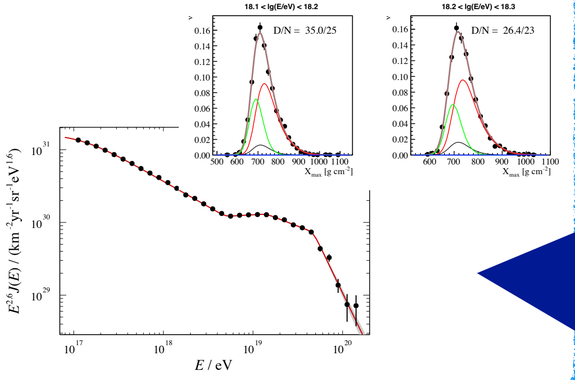

→ **maximum likelihood method**

$$D = D(J) + D(X_{\rm max}) = -2\ln\left(\frac{\mathcal{L}}{\mathcal{L}^{\rm sat}}\right) = -2\ln\left(\frac{\mathcal{L}_J}{\mathcal{L}^{\rm sat}_J}\right) - 2\ln\left(\frac{\mathcal{L}_{X_{\rm max}}}{\mathcal{L}^{\rm sat}_{X_{\rm max}}}\right)$$

[1] R. Aloisio et al, JCAP 11 (2017) 009

The combined fit

CR$_S$ EJECTED BY EG ACCELERATORS

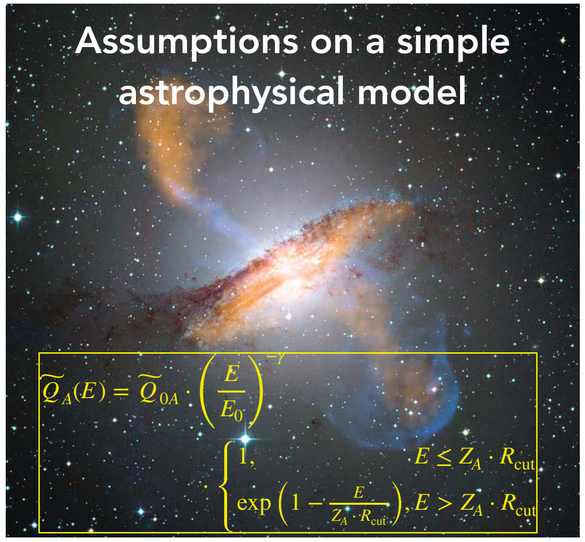

Choice of propagation models for uncertain quantities

PROPAGATION THROUGH THE INTERGALACTIC MEDIUM

SIMPROP

Choice of hadronic interaction model

PRODUCTION OF SHOWERS IN THE ATMOSPHERE

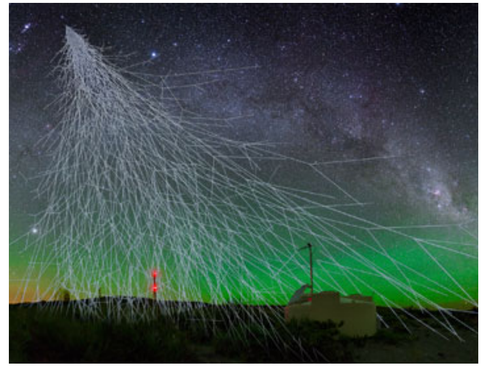

Detector effects are included

COMPARISON WITH THE OBSERVED DATA

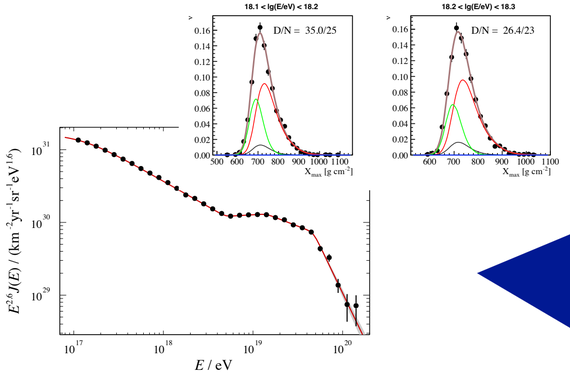

Estimation of free parameters at the escape from sources

[1] R. Aloisio et al, JCAP 11 (2017) 009

The combined fit

CR$_S$ EJECTED BY EG ACCELERATORS

Assumptions on a simple astrophysical model

$$\widetilde{Q}_A(E) = \widetilde{Q}_{0A} \cdot \left(\frac{E}{E_0}\right)^{-\gamma} \cdot \begin{cases} 1, & E \le Z_A \cdot R_{\rm cut} \\ \exp\left(1 - \frac{E}{Z_A \cdot R_{\rm cut}}\right), & E > Z_A \cdot R_{\rm cut} \end{cases}$$

Choice of propagation models for uncertain quantities

PROPAGATION THROUGH THE INTERGALACTIC MEDIUM

SIMPROP

Choice of hadronic interaction model

PRODUCTION OF SHOWERS IN THE ATMOSPHERE

→ CHARACTERISATION OF THE FLUXES AT THE SOURCES (ENERGY SPECTRUM & MASS COMPOSITION)

$$\widetilde{Q}_A(E) = \widetilde{Q}_{0A} \cdot \left(\frac{E}{E_0}\right)^{-\gamma} \cdot \begin{cases} 1, & E \le Z_A \cdot R_{\rm cut} \\ \exp\left(1 - \frac{E}{Z_A \cdot R_{\rm cut}}\right), & E > Z_A \cdot R_{\rm cut} \end{cases}$$

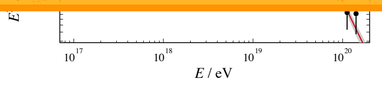

Estimation of free parameters at the escape from sources

Detector effects are included

R. Aloisio et al, JCAP 11 (2017) 009

The reference scenarios

- **Superposition of two (or more) populations to describe the ankle feature**
- Extragalactic components ejected according to a power law with a rigidity dependent cutoff (with different parameters)

Model configuration used for our reference results:

Talys for σ_{pd}, Gilmore model for EBL, EPOS-LHC as hadronic interaction model

J. Koning et al., vol. 769 of American Institute of Physics Conference Series, 2005
R. Gilmore et al., Mon. Not. Roy. Astron. Soc., 422 (2012) 3189
T. Pierog et al., Phys. Rev. C 92 (2015) 034906

The reference scenarios

- **Superposition of two (or more) populations to describe the ankle feature**
- Extragalactic components ejected according to a power law with a rigidity dependent cutoff (with different parameters)

Model configuration used for our reference results:

Talys for σ_{pd}, Gilmore model for EBL, EPOS-LHC as hadronic interaction model

SCENARIO 1 : EXTRAGALACTIC AND GALACTIC POPULATIONS

- **Extragalactic populations with mixed mass composition** dominating at high energy (HE)
- **Extragalactic population of pure protons** dominating at low energy (LE)

  → Possibly produced by decay of neutrons from photodisintegrations of nuclei in the same source environment
- **Galactic additional contribution** at low energy (considered at the Earth → no propagation included)

  → the best fit is given by a nitrogen component extending up to $Z \cdot R_{\rm cut}^{\rm Gal} \approx 2 \cdot 10^{18}$ eV

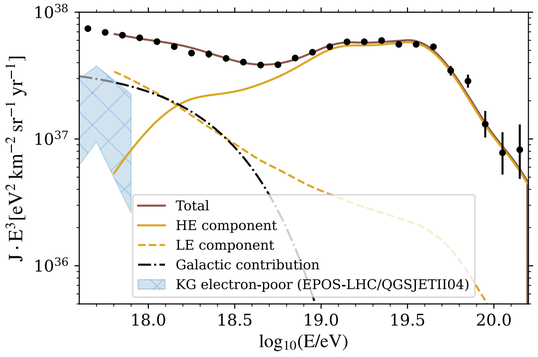

J. Koning et al., vol. 769 of American Institute of Physics Conference Series, 2005
R. Gilmore et al., Mon. Not. Roy. Astron. Soc., 422 (2012) 3189
T. Pierog et al., Phys. Rev. C 92 (2015) 034906

The reference scenarios

- **Superposition of two (or more) populations to describe the ankle feature**
- Extragalactic components ejected according to a power law with a rigidity dependent cutoff (with different parameters)

Model configuration used for our reference results:

Talys for σ_{pd}, Gilmore model for EBL, EPOS-LHC as hadronic interaction model

SCENARIO 1 : EXTRAGALACTIC AND GALACTIC POPULATIONS

- **Extragalactic populations with mixed mass composition** dominating at high energy (HE)
- **Extragalactic population of pure protons** dominating at low energy (LE)

  → Possibly produced by decay of neutrons from photodisintegrations of nuclei in the same source environment
- **Galactic additional contribution** at low energy (considered at the Earth → no propagation included)

  → the best fit is given by a nitrogen component extending up to $Z \cdot R_{\rm cut}^{\rm Gal} \approx 2 \cdot 10^{18}$ eV

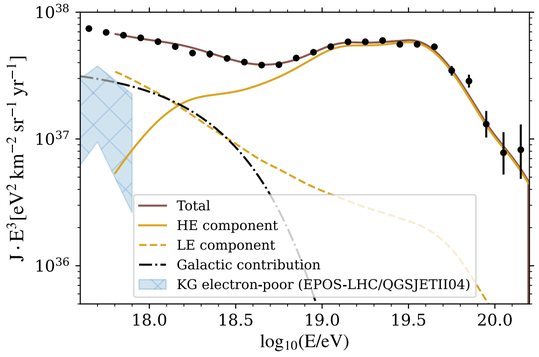

SCENARIO 2 : TWO MIXED EXTRAGALACTIC POPULATIONS

- **Extragalactic populations with mixed mass composition** dominating at high energy (HE)
- **Extragalactic population with mixed mass composition** dominating at low energy (LE)

  → produced by two different populations of sources

  → Galactic contributions are subdominant in this energy range

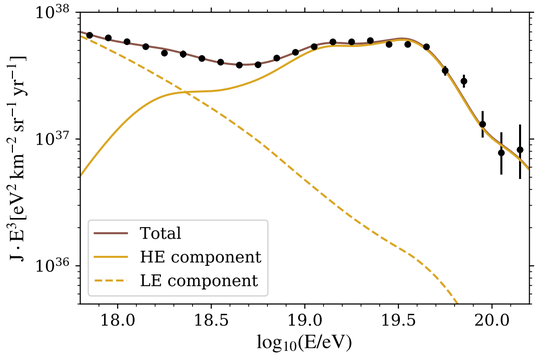

J. Koning et al., vol. 769 of American Institute of Physics Conference Series, 2005
R. Gilmore et al., Mon. Not. Roy. Astron. Soc., 422 (2012) 3189
T. Pierog et al., Phys. Rev. C 92 (2015) 034906

Results in the reference scenarios

Some common findings between the two scenarios

Generation rate at the sources

$$\widetilde{Q}_A(E) = \widetilde{Q}_{0A} \cdot \left(\frac{E}{E_0}\right)^{-\gamma} \cdot \begin{cases} 1, & E \le Z_A \cdot R_{\rm cut} \\ \exp\left(1 - \frac{E}{Z_A \cdot R_{\rm cut}}\right), & E > Z_A \cdot R_{\rm cut} \end{cases}$$

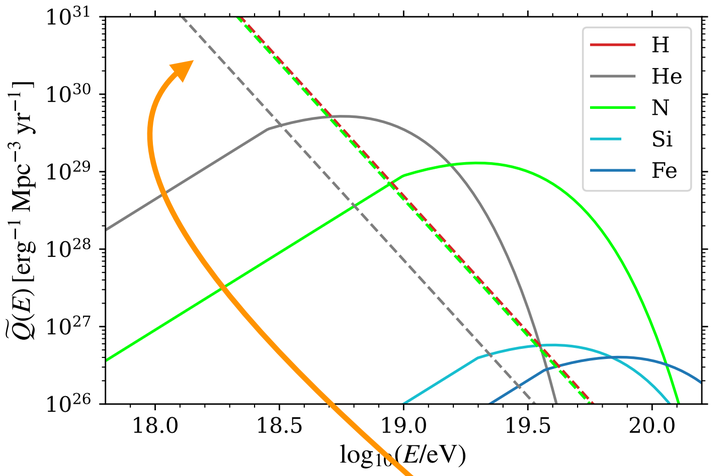

Plots refer only to Scenario 2 for figurative purposes

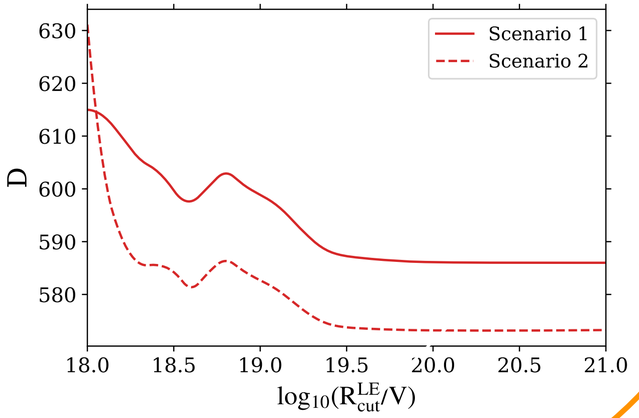

Mass composition at the Earth

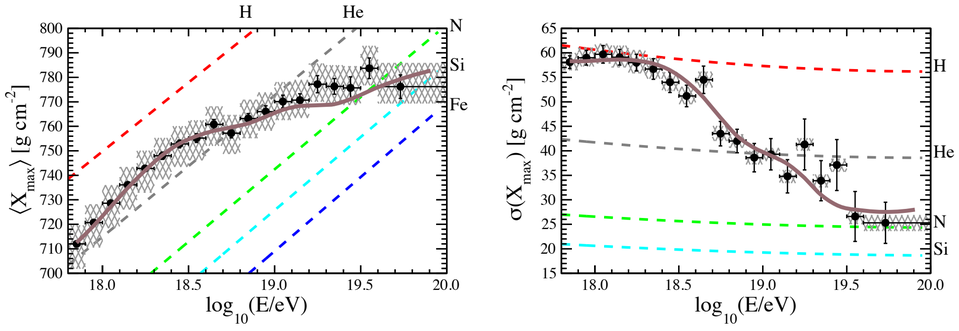

LE component:

- Very soft energy spectrum ($\gamma > 3$)
- Very high rigidity cutoff (degenerate fit for $R^{LE}_{cut} \gg 10^{19.5}$eV)

Energy spectrum at the Earth

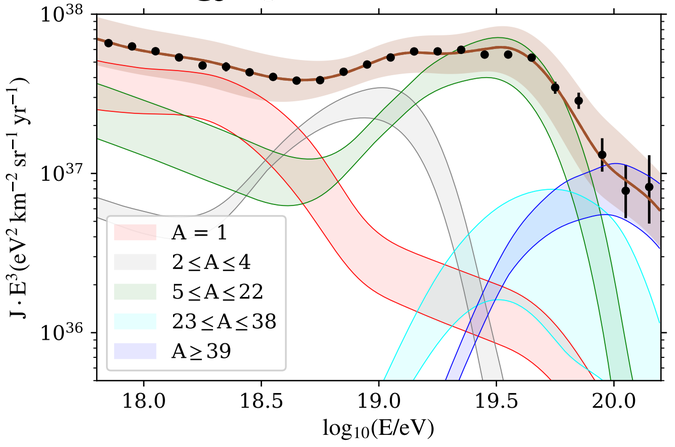

Results in the reference scenarios

Some common findings between the two scenarios

Generation rate at the sources

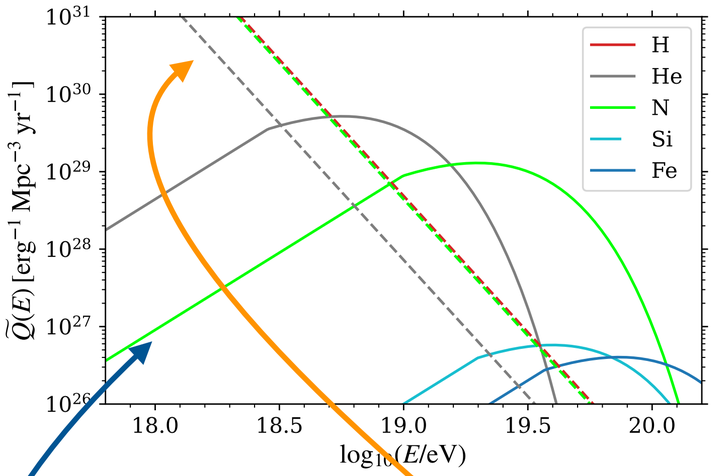

$$\widetilde{Q}_A(E) = \widetilde{Q}_{0A} \cdot \left(\frac{E}{E_0}\right)^{-\gamma} \cdot \begin{cases} 1, & E \le Z_A \cdot R_{\rm cut} \\ \exp\left(1 - \frac{E}{Z_A \cdot R_{\rm cut}}\right), & E > Z_A \cdot R_{\rm cut} \end{cases}$$

Plots refer only to Scenario 2 for figurative purposes

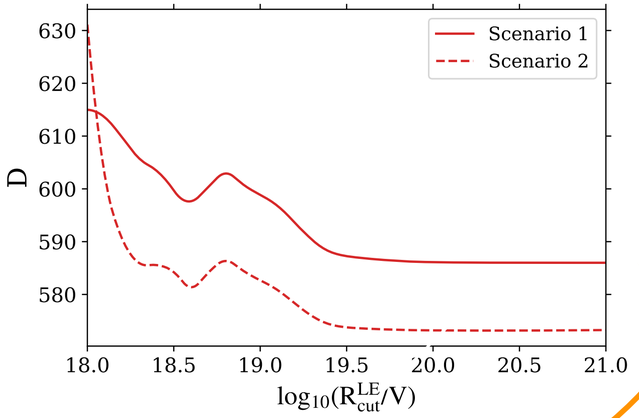

Mass composition at the Earth

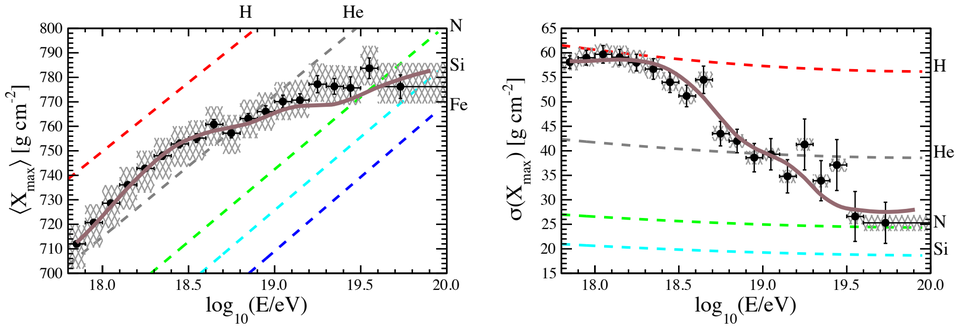

LE component:

- Very soft energy spectrum ($\gamma > 3$)
- Very high rigidity cutoff (degenerate fit for $R_{cut}^{LE} \gg 10^{19.5}$eV)

HE component:

- Very hard energy spectrum ($\gamma < 0$) required to describe the very pronounced spectral features and narrow X_{max} distributions.
- Low rigidity cutoff <u>but</u> not low enough to make propagation effects negligible

Energy spectrum at the Earth

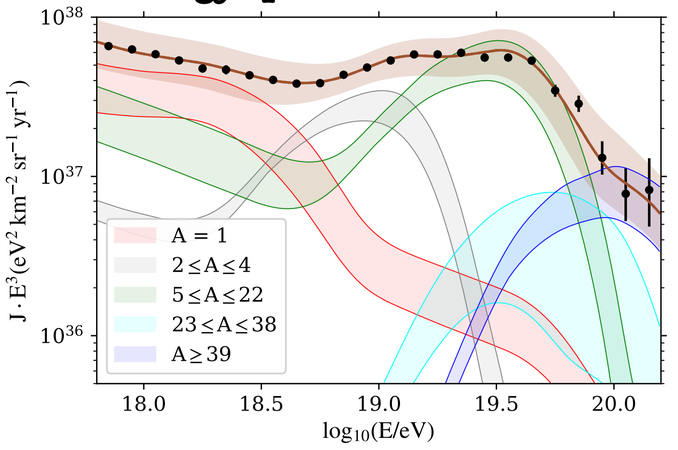

Results in the reference scenarios

Some common findings between the two scenarios

Generation rate at the sources

$$\widetilde{Q}_A(E) = \widetilde{Q}_{0A} \cdot \left(\frac{E}{E_0}\right)^{-\gamma} \cdot \begin{cases} 1, & E \le Z_A \cdot R_{\rm cut} \\ \exp\left(1 - \frac{E}{Z_A \cdot R_{\rm cut}}\right), & E > Z_A \cdot R_{\rm cut} \end{cases}$$

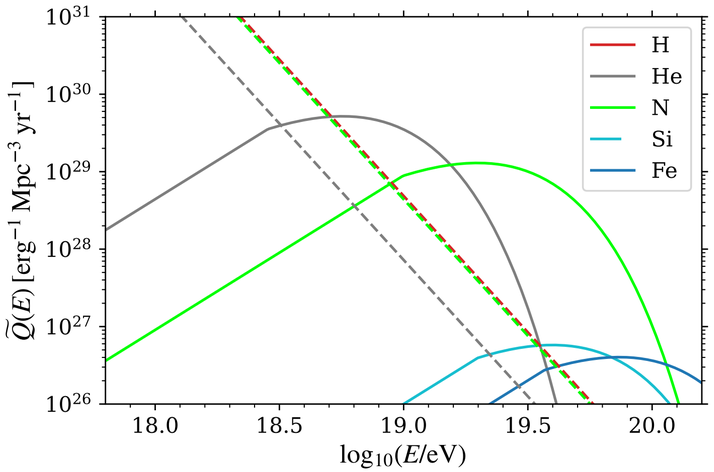

Plots refer only to Scenario 2 for figurative purposes

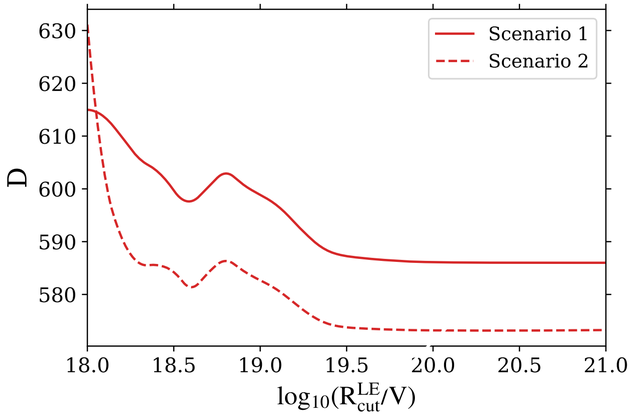

Mass composition at the Earth

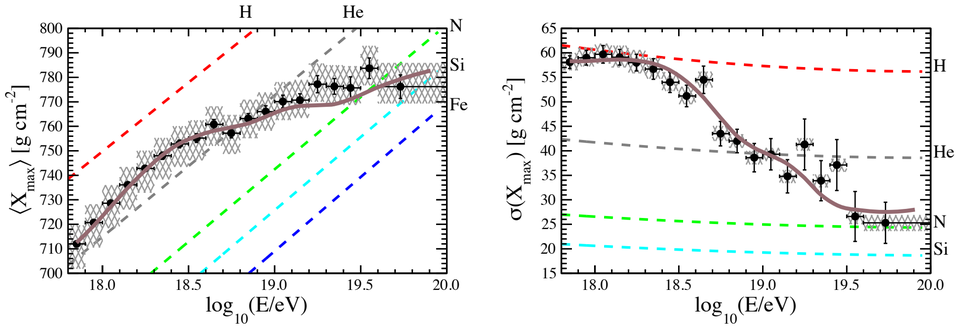

- The **ankle** is described by the superposition of the two components
- The **instep** is given by the interplay between the He and N components
- The **suppression** is given by a combined effect of propagation and maximum energy at the acceleration

Energy spectrum at the Earth

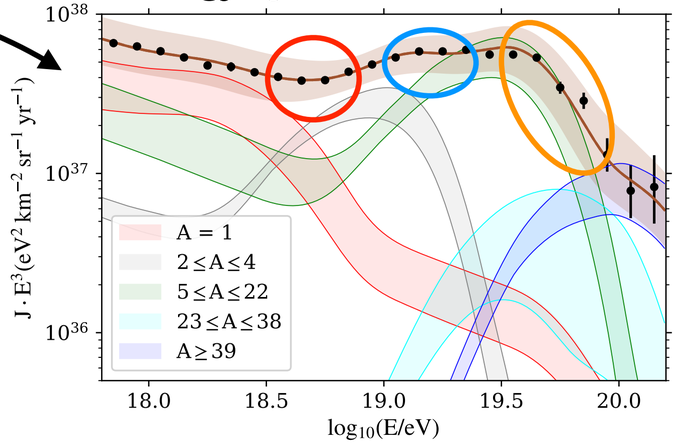

Results in the reference scenarios

Mixed and increasingly heavier mass composition of the HE component

- No mass composition information at the highest energies
  → fit based on the shape of the energy spectrum

Mixture of H+N at LE (below the ankle) in both scenarios

In Scenario 1 the contribution heavier than protons is Galactic at LE:

- Models with Galactic Fe/Si right below the ankle are strongly disfavoured
- **a N-dominated composition is preferred**
  → possible presence of an additional Galactic component extending up to higher energies

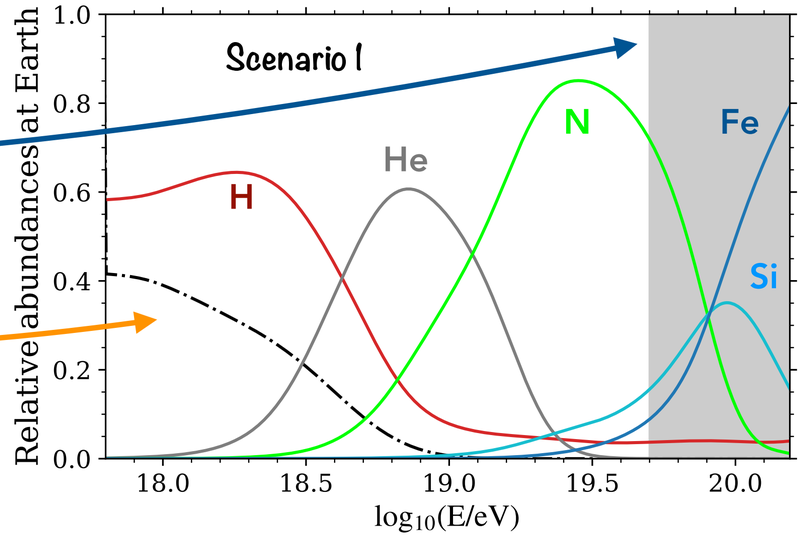

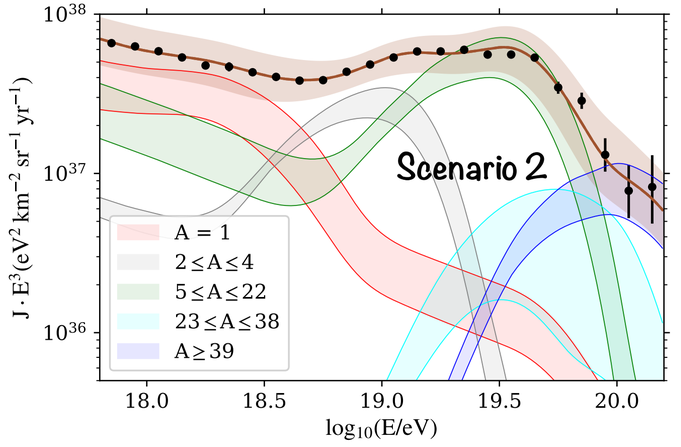

Results in the reference scenarios

Mixed and increasingly heavier mass composition of the HE component

- No mass composition information at the highest energies
  → fit based on the shape of the energy spectrum

Mixture of H+N at LE (below the ankle) in both scenarios

In Scenario 1 the contribution heavier than protons is Galactic at LE:

- Models with Galactic Fe/Si right below the ankle are strongly disfavored
- **a N-dominated composition is preferred**
  → possible presence of an additional Galactic component extending up to higher energies

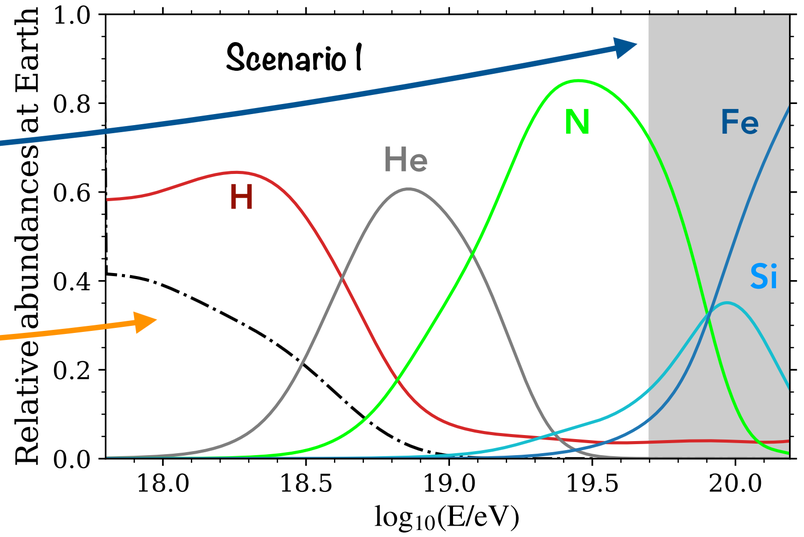

- **Experimental uncertainties are the dominant ones** (mainly from the X_{max} scale)
- The **systematic uncertainties do not spoil our conclusions** in the reference scenarios

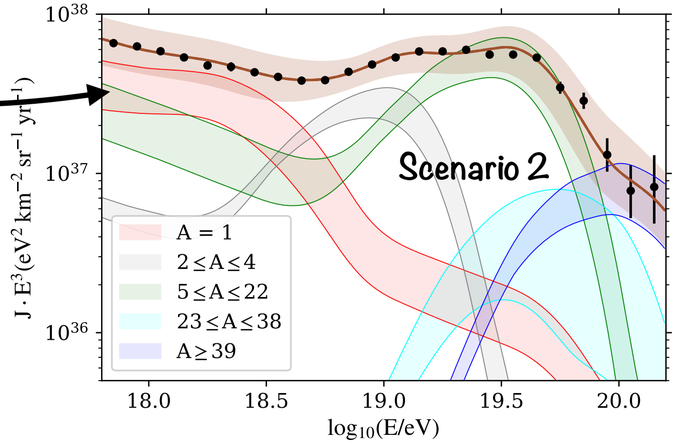

Results in the reference scenarios

Mixed and increasingly heavier mass composition of the HE component

- No mass composition information at the highest energies
  → fit based on the shape of the energy spectrum

Mixture of H+N at LE (below the ankle) in both scenarios

In Scenario 1 the contribution heavier than protons is Galactic at LE:

- Models with Galactic Fe/Si right below the ankle are strongly disfavored
- **a N-dominated composition is preferred**
  → possible presence of an additional Galactic component extending up to higher energies

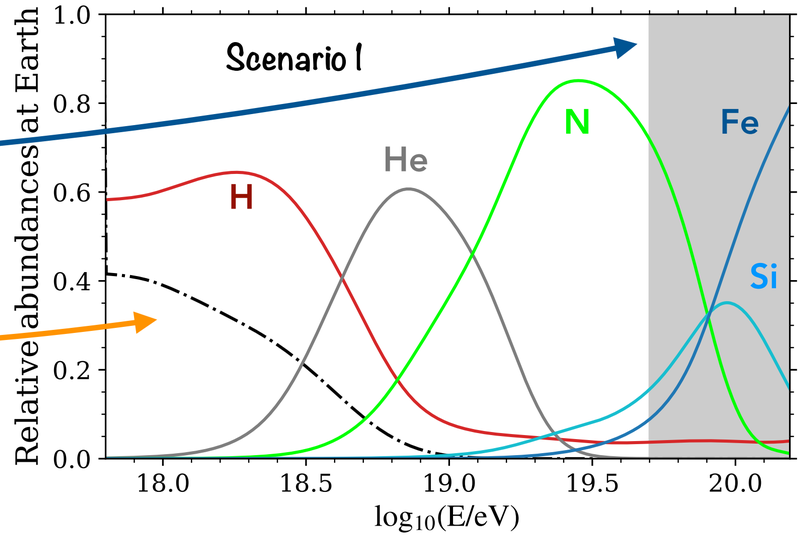

- **Experimental uncertainties are the dominant ones** (mainly from the X_{max} scale)
- The **systematic uncertainties do not spoil our conclusions** in the reference scenarios

It is not possible to choose a favored scenario in terms of the deviance

- The **differences are encompassed within the systematic uncertainties**
- In Scenario 2, photodisintegration is negligible for the LE component
  → light-to-intermediate masses (similar to the one at the sources)
- Further investigation of the Galactic-to-extragalactic transition region is necessary

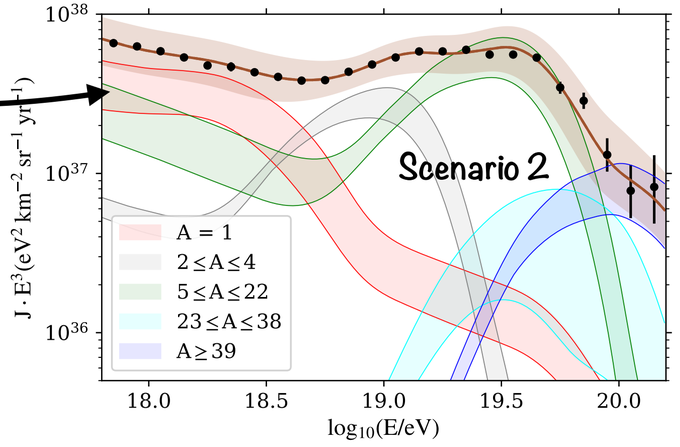

Cosmological evolution of sources

- Three alternative models for the **evolution of the source emissivity, parameterized as** $\propto (1+z)^m$
  → m=-3, m=+3, m=+5 (m=0 was used in the reference scenarios)
- The behaviour at z>1 has only a negligible impact on the LE component (no impact on the HE one)
- All the possible combinations have been tested

Cosmological evolution of sources

- Three alternative models for the **evolution of the source emissivity, parameterized as** $\propto (1+z)^m$
  → m=-3, m=+3, m=+5 (m=0 was used in the reference scenarios)
- The behaviour at z>1 has only a negligible impact on the LE component (no impact on the HE one)
- All the possible combinations have been tested

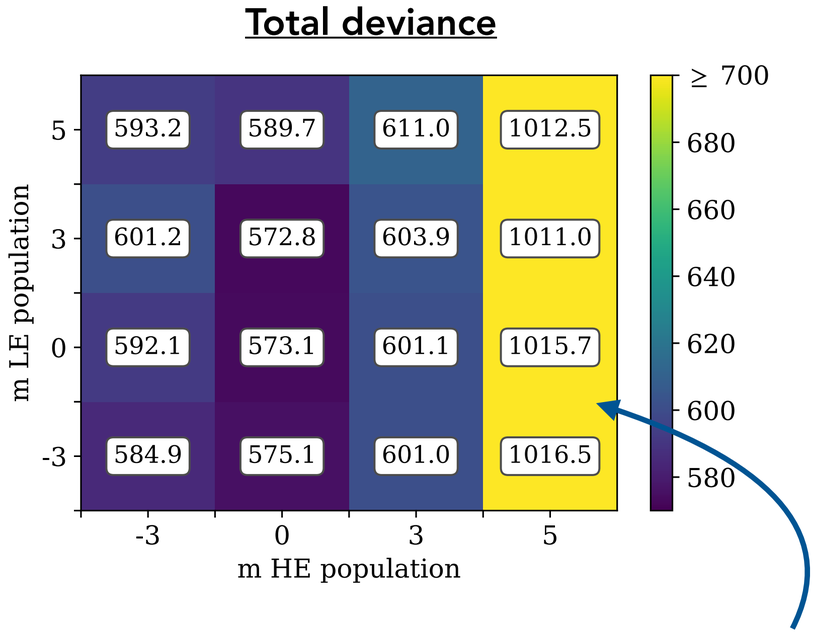

Strong source evolution for the HE is disfavoured

(too many secondary particles at the ankle)

Cosmological evolution of sources

- Three alternative models for the **evolution of the source emissivity, parameterized as** $\propto (1+z)^m$
  → m=-3, m=+3, m=+5 (m=0 was used in the reference scenarios)
- The behaviour at z>1 has only a negligible impact on the LE component (no impact on the HE one)
- All the possible combinations have been tested

Total deviance

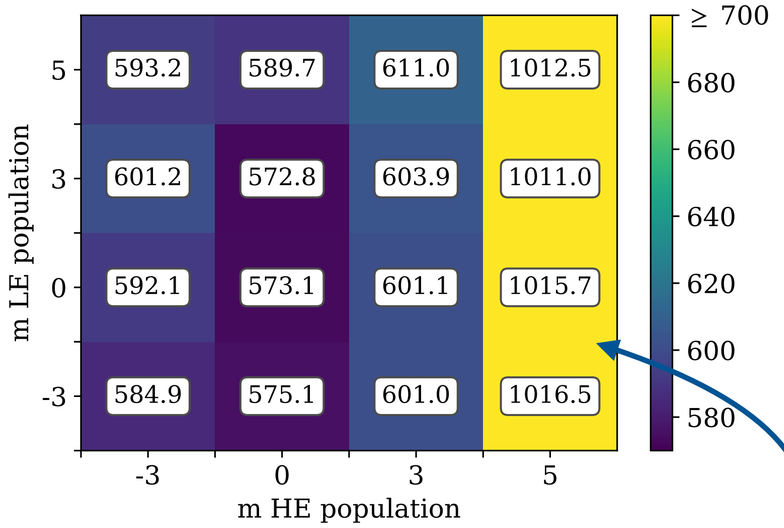

Strong source evolution for the HE is disfavoured

(too many secondary particles at the ankle)

Neutrinos fluxes for a strong evolution of the LE component

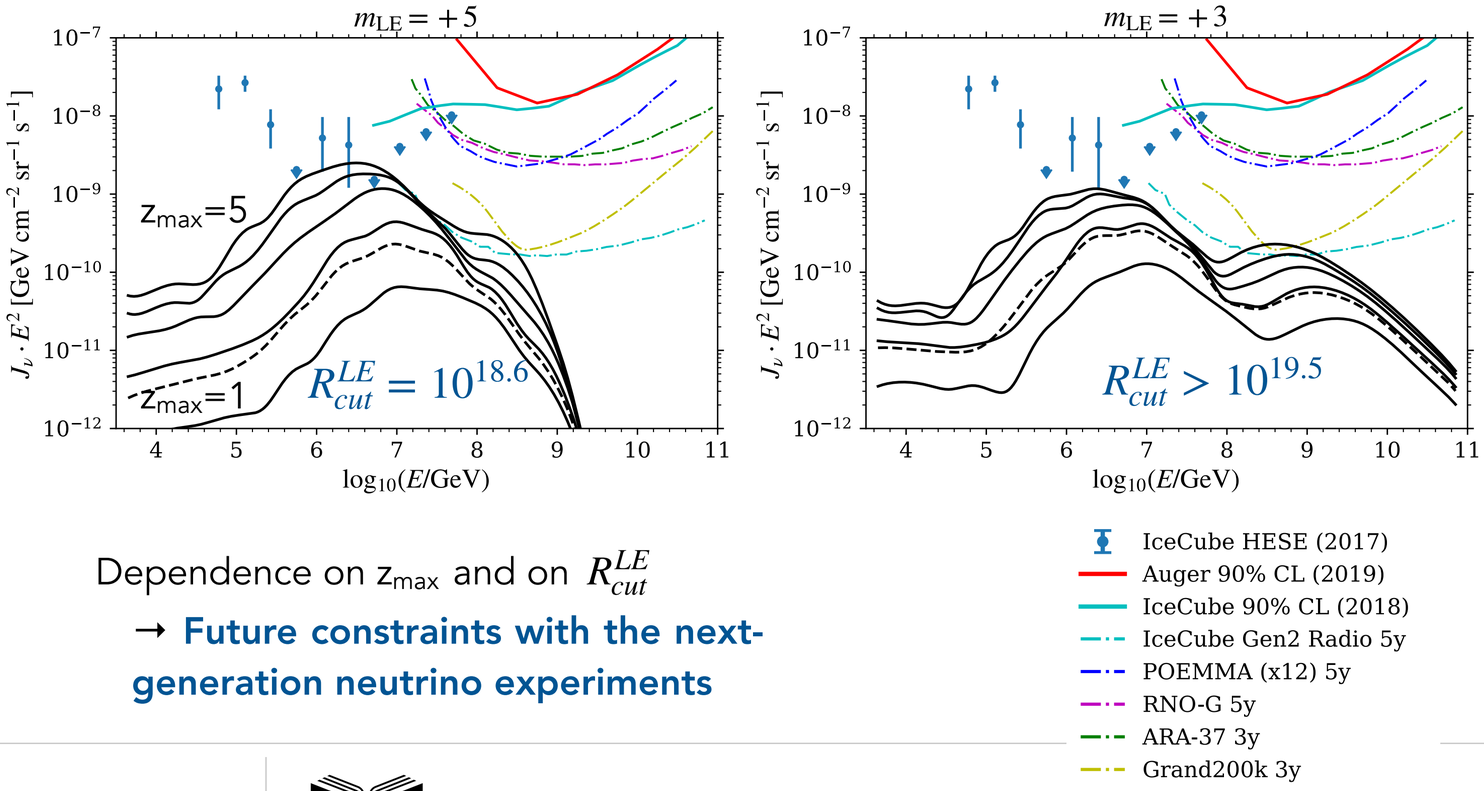

Dependence on $z_{\rm max}$ and on R_{cut}^{LE}

→ **Future constraints with the next-generation neutrino experiments**

Constraints from neutrino fluxes

- Preliminary analysis performing a thicker scan over the ($z_{\max}$, m) parameter space (both $z_{\max}$ and m from 3.0 to 5.0 with a 0.2 step)

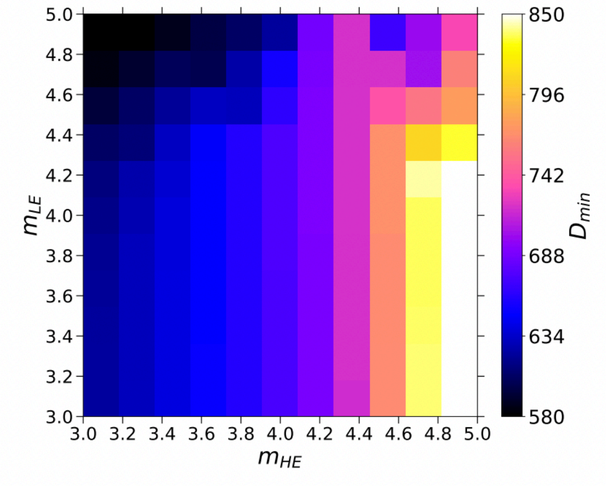

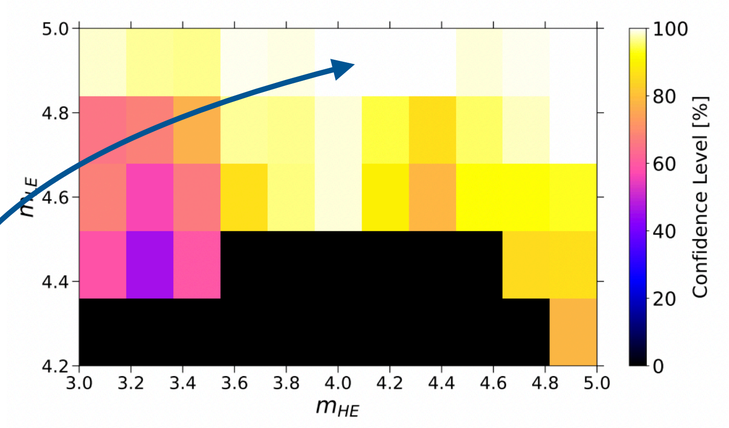

Confidence level associated to the predicted cosmogenic neutrinos

- Some combinations of source evolutions are excluded at the 90% C.L. → e.g. for $m_{\mathrm{HE}} = 4.0$, $m_{\mathrm{LE}} \geq 4.6$ is excluded

  → **additional constraints on $m_{\mathrm{HE}}/m_{\mathrm{LE}}$ from the cosmogenic neutrino fluxes**

Constraints from neutrino fluxes

- Preliminary analysis performing a thicker scan over the ($z_{\max}$, m) parameter space (both $z_{\max}$ and m from 3.0 to 5.0 with a 0.2 step)

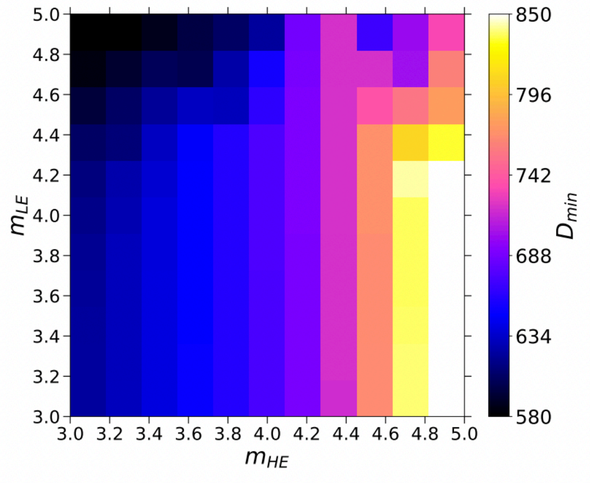

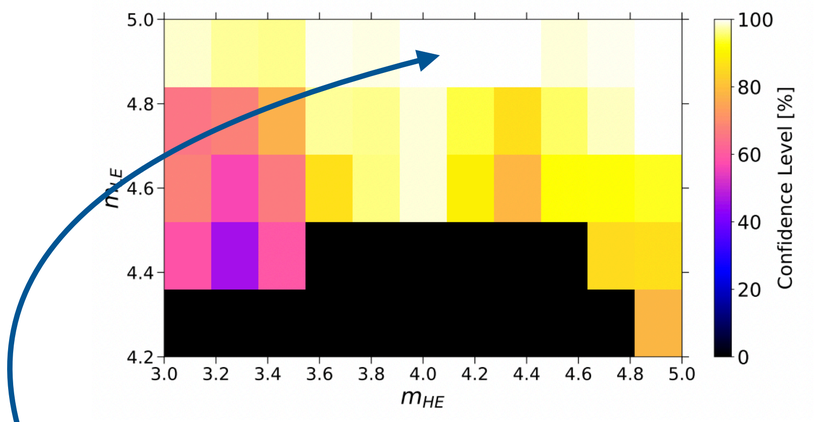

Confidence level associated to the predicted cosmogenic neutrinos

- Some combinations of source evolutions are excluded at the 90% C.L. → e.g. for $m_{\mathrm{HE}} = 4.0$, $m_{\mathrm{LE}} \geq 4.6$ is excluded

  → **additional constraints on $m_{\mathrm{HE}}/m_{\mathrm{LE}}$ from the cosmogenic neutrino fluxes**

- Cosmogenic neutrinos are mostly produced by the proton component
- **Investigation on the fraction of protons compatible with data:**
  - ➡ Fixed spectral parameters (above the ankle)
  - ➡ The expected spectrum is re-scaled by F_p (proton fraction)

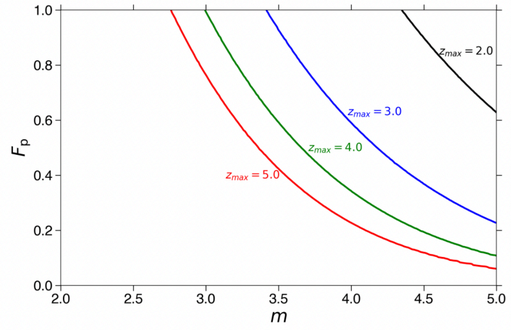

Around the ankle F_p is ~20%

→ exclusion of source classes with $z_{\max} = 5.0$ and $m > 4.0$

Effect of the extragalactic magnetic field

- Preliminary analysis including the "**magnetic horizon effect**" on the **HE component**

  → in presence of extragalactic magnetic fields, if the inter-source distance d_s is large enough (density smaller than $10^{-4}\,\mathrm{Mpc}^{-3}$), low-energy particles cannot reach the Earth even from the closest sources

  → **energy spectrum suppressed at low energy**

- The inter-source distance for the LE component is assumed to be small → negligible effect on it

Effect of the extragalactic magnetic field

- Preliminary analysis including the "**magnetic horizon effect**" on the **HE component**

  → in presence of extragalactic magnetic fields, if the inter-source distance d_s is large enough (density smaller than $10^{-4}\,\mathrm{Mpc}^{-3}$), low-energy particles cannot reach the Earth even from the closest sources

  → **energy spectrum suppressed at low energy**

- The inter-source distance for the LE component is assumed to be small → negligible effect on it

✦ Different steepness of the cutoff are explored ($\Delta = 1,2,3$)

✦ No source evolution or SFR-like source evolution for the LE component

✦ Energy-dependent suppression factor **G(x)**

$$J(E) = \sum_A J_{0A}\left(\frac{E}{E_0}\right)^{-\gamma} \mathrm{sech}\left(\frac{E}{Z_A R_{\mathrm{cut}}}\right)^{\Delta}$$

$$J(E) \equiv G(E/E_{\mathrm{crit}}) J_{B=0}(E),$$

$$X_{\mathrm{s}} = d_{\mathrm{s}}/\sqrt{r_H L_{\mathrm{coh}}}$$

$$G(x) = \exp\left[-\left(\frac{a\,X_{\mathrm{s}}}{x + b\,(x/a)^{\beta}}\right)^{\alpha}\right]$$

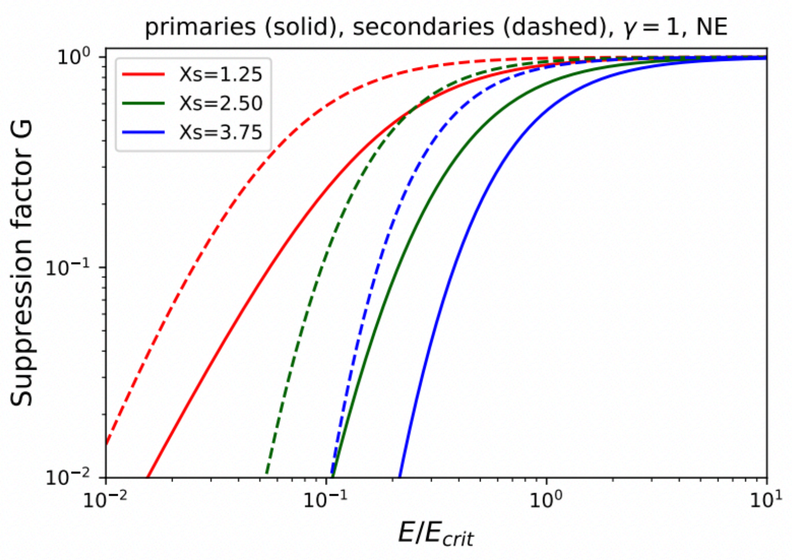

$\Delta = 1$ is equivalent to the reference scenarios

Effect of the extragalactic magnetic field

- Preliminary analysis including the "**magnetic horizon effect**" on the **HE component**

  → in presence of extragalactic magnetic fields, if the inter-source distance d_s is large enough (density smaller than $10^{-4}\,\mathrm{Mpc}^{-3}$), low-energy particles cannot reach the Earth even from the closest sources

  → **energy spectrum suppressed at low energy**

- The inter-source distance for the LE component is assumed to be small → negligible effect on it

EPOS-LHC

$X_s = 2.5$	NE–NE						SFR–NE					
Δ	γ_H	R^H_{cut} [EeV]	γ_L	R^L_{cut} [EeV]	R_{crit} [EeV]	D (N=353)	γ_H	R^H_{cut} [EeV]	γ_L	R^L_{cut} [EeV]	R_{crit} [EeV]	D (N=353)
1	−2.2	1.3	3.5	100	0.4	572	−2.1	1.4	3.2	100	0.0	578
2	1.0	6.2	3.6	100	3.4	586	1.1	6.2	3.3	100	3.7	588
3	1.4	7.6	3.7	100	3.3	615	1.5	7.6	3.4	100	3.5	617
no EGMF				NE–NE						SFR–NE		
1	−2.2	1.4	3.5	100	—	572	−2.1	1.4	3.2	100	—	578
2	0.2	5.8	3.6	100	—	605	0.2	5.8	3.4	100	—	607
3	0.6	7.4	3.8	100	—	651	0.6	7.4	3.5	100	—	652

Magnetic field suppression effect for X_s=2.5 (fixed)

- ✦ **In presence of a steep cutoff ($\Delta = 2,3$) the magnetic field suppression improves the fit and the spectrum softens**
- ✦ The effect on the spectral index increases with X_s → magnetic fields could be responsible for the hardness of the spectrum
- ✦ **<u>But</u> the lowest deviance is obtained or $\Delta = 1$ and the suppression has no significant effect on the results**

Conclusions

Main results of the combined fit across the ankle:

- Simple astrophysical **model with two extragalactic components (with or without a Galactic contribution at LE)**
  → description of the spectral features (ankle, instep, suppression)
  → **similar results** in terms of deviance **in the two scenarios**
- **Galactic component** at LE (if present) : **composition heavier than N strongly disfavoured**
- The systematic uncertainties do not spoil our conclusions
- **Very strong source evolution (m=5) for the HE component is excluded by the fit results**
- The cosmogenic neutrino fluxes in some scenarios may reach the sensitivity of next-generation experiments

Preliminary results from recent on-going analyses:

- Some **combinations of source evolutions (with strong evolution for the LE component)** are excluded by the predictions of cosmogenic neutrinos
- The **magnetic horizon effect softens the spectrum of the HE component** in some scenarios → relationship between magnetic fields and the hardness of the HE energy spectrum to be further investigated

The Pierre Auger Collaboration, JCAP05(2023)024
C. Petrucci for the Pierre Auger Collaboration, PoS(ICRC2023)1520
J.Gonzalez for the Pierre Auger Collaboration, PoS(ICRC2023)288

Outlook

- Further investigations related to the previously mentioned on-going analyses
- Update of the X_{max} analysis including also data from **low-energy extension of Auger** (HEAT → High-Elevation Auger Telescopes) in progress
  → *further insights on the Galactic-to-extragalactic transition region*
- Additional information **including arrival directions** in the fit
  → study with a combined fit above the ankle presented at the ICRC2023 [PoS(ICRC2023)258]
- Inclusion of mass composition estimates with machine learning techniques on SD data
- Improvement of the **mass composition information at the highest energies** from the detector upgrade (**AugerPrime**)
  → same analysis could be performed with *much more statistics*
  → *mass composition information at the high-energy suppression*

THANK YOU FOR YOUR ATTENTION!

Back-up slides

Measurements of the energy and mass composition

Surface Detector (SD)

- Duty cycle: ~100%
- Measurement of the lateral distribution of signals

Hybrid events = observed by both detectors

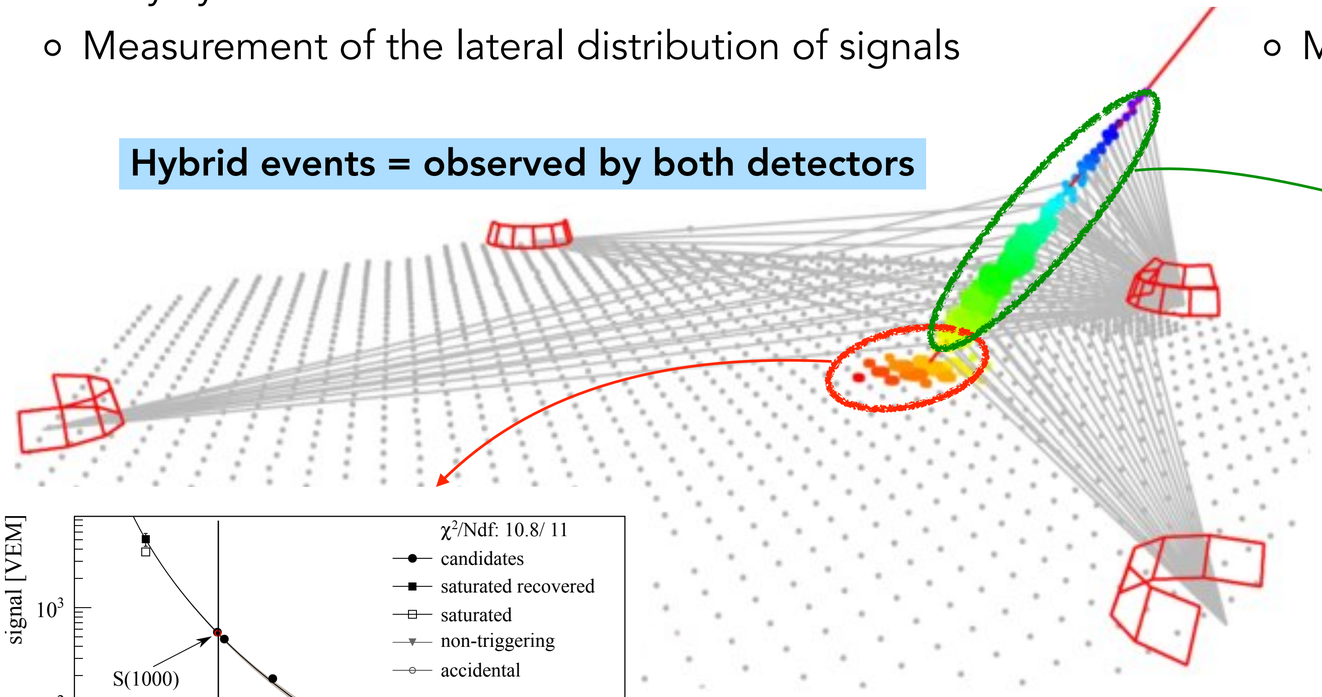

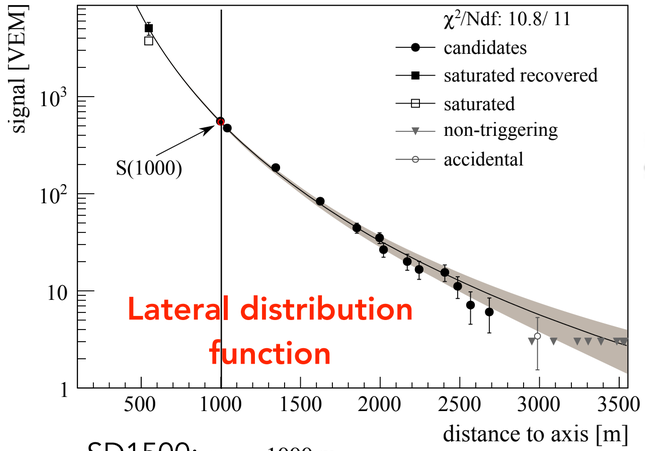

Lateral distribution function

SD1500: $r_{opt} = 1000$ m

SD750 (Infill): $r_{opt} = 450$ m

Estimator $S(r_{opt})$ = shower size at a distance r_{opt} from the core

$$S(r) \propto r^{\beta}(r + r_M)^{\beta+\gamma} \rightarrow S(r_{opt})$$

Fluorescence Detector (FD)

- Duty cycle: ~15%
- Measurement of the longitudinal profile

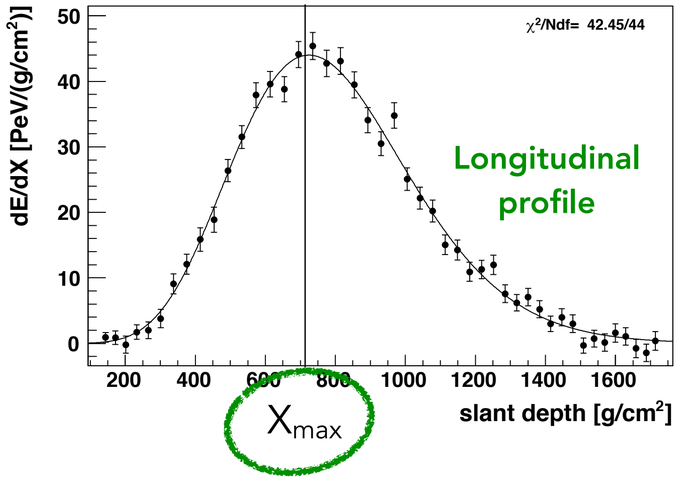

Depth of shower maximum

$$E_{cal} = \int \frac{dE}{dX} dX$$

Calorimetric energy

- X_{max} used as a **mass composition estimator for the FD events**
- **Energy of all the SD events** obtained through the calibration between S and E_{cal} with the hybrid events

Astrophysical model

Generic population of extragalactic sources

- population of identical sources
- uniform distribution (except for a local overdensity for $d < 30\ \mathrm{Mpc}$)
- ejection of **n representative nuclear species A**, chosen among ^{1}H, ^{4}He, ^{14}N, ^{28}Si, ^{56}Fe

Generation rate at the sources for each mass A (number of nuclei ejected per unit of energy, volume and time) **:**

$$\widetilde{Q}_A(E) = \widetilde{Q}_{0A} \cdot \left(\frac{E}{E_0}\right)^{-\gamma} \cdot \begin{cases} 1, & E \le Z_A \cdot R_{\mathrm{cut}}; \\ \exp\left(1 - \frac{E}{Z_A \cdot R_{\mathrm{cut}}}\right), & E > Z_A \cdot R_{\mathrm{cut}}, \end{cases}$$

Characterizing the fluxes escaping the source environment → parameters estimated in the fit

- Spectral parameters γ, R_{cut}
- n partial normalisations $\widetilde{Q}_{0A}$

$$\widetilde{Q}_{0A} \longrightarrow I_A = \frac{\int_{E_{\mathrm{min}}}^{\infty} E \cdot \widetilde{Q}_A(E)\, dE}{\mathscr{L}_0}$$

Fractions of the total emissivity of sources above $E_{min} = 10^{17.8}$ eV

$$with\ \ \mathscr{L}_0 = \sum_A \int_{E_{\mathrm{min}}}^{\infty} E \cdot \widetilde{Q}_A(E)\, dE$$

Emissivity of a population: total energy ejected per unit of comoving volume and time

expressed in $\mathrm{erg} \cdot \mathrm{Mpc}^{-3} \cdot \mathrm{yr}^{-1}$

Propagation model

Propagation through the IGM and the Earth's atmosphere

- **SimProp simulations** for the **propagation in the IGM** → **model for the photo-disintegration cross sections $\sigma_{\rm pd}$**
  → **model for the EBL spectrum and evolution**

  - Adiabatic energy losses (expansion of the Universe) $$-\left(\frac{1}{E}\frac{dE}{dt}\right)_{ad} = H_0\sqrt{(1+z)^3\Omega_m + \Omega_\Lambda}$$
  - Interactions of nuclei with background photons (EBL, CMB)
    - Photo-pion production $N + \gamma \rightarrow N + \pi^0 \ / \ N + \pi^\pm$
    - Pair production $N + \gamma \rightarrow N + e^+ + e^-$
    - Photo-disintegration $(A, Z) + \gamma \rightarrow (A - n, Z - n') + nN$

- **Hadronic interaction model** for the **propagation in the atmosphere**
- 1D propagation → intergalactic magnetic fields are here neglected

Model configuration used for our reference results:
Talys for $\sigma_{\rm pd}$, Gilmore model for EBL, EPOS-LHC as hadronic interaction model

J. Koning et al., vol. 769 of American Institute of Physics Conference Series, 2005
R. Gilmore et al., Mon. Not. Roy. Astron. Soc., 422 (2012) 3189
T. Pierog et al., Phys. Rev. C 92 (2015) 034906

Fit procedure

Combined fit of the energy spectrum and X_{max} distributions above $\sim 6 \times 10^{17}\mathrm{eV}$

→ compare simulated and measured fluxes at the Earth with the **maximum likelihood method**

$$D = D(J) + D(X_{\mathrm{max}}) = -2\ \ln\left(\frac{\mathscr{L}}{\mathscr{L}^{\mathrm{sat}}}\right) = -2\ \ln\left(\frac{\mathscr{L}_{\mathrm{J}}}{\mathscr{L}_{\mathrm{J}}^{\mathrm{sat}}}\right) - 2\ \ln\left(\frac{\mathscr{L}_{X_{\mathrm{max}}}}{\mathscr{L}_{X_{\mathrm{max}}}^{\mathrm{sat}}}\right)$$

- **Energy spectrum** → Gaussian distributions

$$L_{\mathrm{J}} = \prod_i \frac{1}{\sqrt{2\pi\sigma_i^2}} \exp\left(-\frac{(J_i^{\mathrm{obs}} - J_i^{\mathrm{mod}})^2}{2\sigma_i^2}\right),$$

observed unfolded flux (detector effects)

expected simulated flux

- **X_{max} distributions** → multinomial distributions

$$L_{X_{\mathrm{max}}} = \sum_i n_i^{\mathrm{obs}}! \sum_j \frac{1}{k_{i,j}^{\mathrm{obs}}!} \left(G_{i,j}^{\mathrm{mod}}\right)^{k_{i,j}^{\mathrm{obs}}}$$

observed events

model probability

i = $\log_{10}$(E) bin, j = X_{max} bin

(Gumbel distribution + detector effects)

$$D = D(J) + D(X_{\mathrm{max}}) = \sum_i \frac{(J_i^{\mathrm{obs}} - J_i^{\mathrm{mod}})^2}{\sigma_i^2} + 2 \cdot \sum_i \sum_{k_{i,j}^{\mathrm{obs}}} k_{i,j}^{\mathrm{obs}} \cdot \ln\left(\frac{k_{i,j}^{\mathrm{obs}}}{n_i^{\mathrm{obs}} \cdot G_{i,j}^{\mathrm{mod}}}\right)$$

→ The observed and simulated fluxes are compared by minimising the deviance D

Results in the reference scenarios

Some common findings between the two scenarios:

Very hard energy spectrum for the HE extragalactic component

- little overlap between different masses
  → description of very pronounced spectral features and narrow X_{max} distributions.
- Considering only the extragalactic propagation
  → energy-dependent effects in the source environment are not included
- "Magnetic horizon" effect
  → observed harder spectrum because of the suppression of the low-energy fluxes

	Scenario 1		Scenario 2	
Galactic contribution (at Earth)	pure N		—	
$J_0^{\rm Gal}$ [$\rm eV^{-1}\cdot km^{-2}\cdot sr^{-1}\cdot yr^{-1}$]	$(1.06 \pm 0.04)\cdot 10^{-13}$		—	
$\log_{10}(R_{\rm cut}^{\rm Gal}/{\rm V})$	17.48 ± 0.02		—	
EG components (at the escape)	LE	HE	LE	HE
$\mathcal{L}_0$ [$10^{44}\cdot \rm erg\cdot Mpc^{-3}\cdot yr^{-1}$] *	6.54 ± 0.36	5.00 ± 0.35	11.35 ± 0.15	5.07 ± 0.06
γ	3.34 ± 0.07	-1.47 ± 0.13	3.52 ± 0.03	-1.99 ± 0.11
$\log_{10}(R_{\rm cut}/{\rm V})$	> 19.3	18.19 ± 0.02	> 19.4	18.15 ± 0.01
$I_{\rm H}$ (%)	100 (fixed)	0.0 ± 0.0	48.7 ± 0.3	0.0 ± 0.0
$I_{\rm He}$ (%)	—	24.5 ± 3.0	7.3 ± 0.4	23.6 ± 1.6
$I_{\rm N}$ (%)	—	68.1 ± 5.0	44.0 ± 0.4	72.1 ± 3.3
$I_{\rm Si}$ (%)	—	4.9 ± 3.9	0.0 ± 0.0	1.3 ± 1.3
$I_{\rm Fe}$ (%)	—	2.5 ± 0.2	0.0 ± 0.0	3.1 ± 1.3
D_J (N_J)	48.6 (24)		56.6 (24)	
$D_{X_{\rm max}}$ ($N_{X_{\rm max}}$)	537.4 (329)		516.5 (329)	
D (N)	586.0 (353)		573.1 (353)	

* from $E_{\rm min} = 10^{17.8}$ eV.

Generation rate at the sources

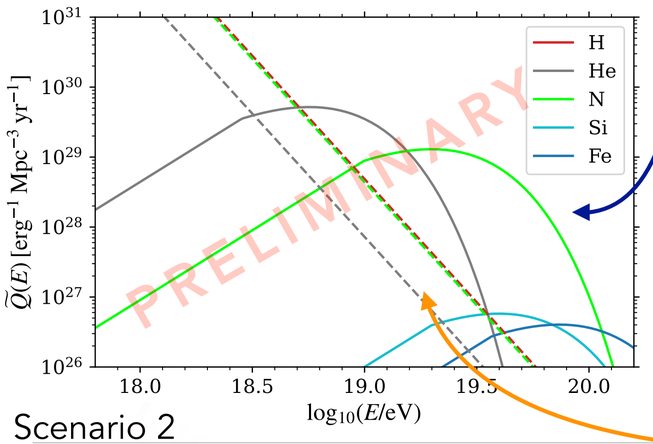

Energy spectrum at the Earth

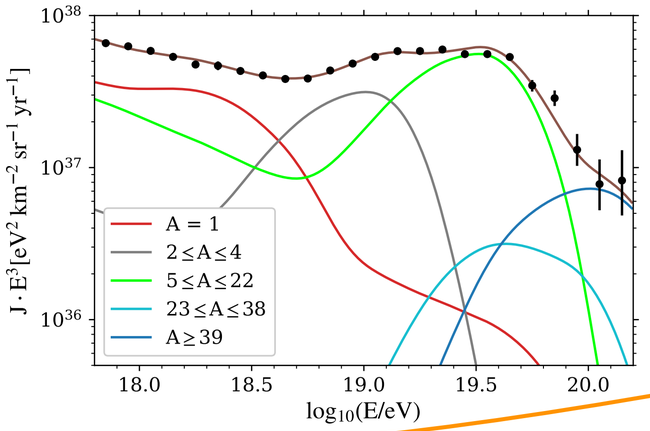

Scenario 2

Very soft energy spectrum for the LE extragalactic component

Possible explanation:

- Sources with different maximal energies (not identical)
  → the energy spectrum of each source may be less steep

Results in the reference scenarios

Some common findings between the two scenarios:

Low rigidity cutoff of the HE component

- It affects the observed fluxes (< $10^{18.5}$ eV)

  → <u>but</u> not low enough to make propagation effects negligible

Mixed mass composition of the HE component

- No mass composition information at the highest energies

  → fit based on the shape of the energy spectrum

	Scenario 1		Scenario 2	
Galactic contribution (at Earth)	pure N		—	
$J_0^{\rm Gal}$ [$\rm eV^{-1}\cdot km^{-2}\cdot sr^{-1}\cdot yr^{-1}$]	$(1.06 \pm 0.04)\cdot 10^{-13}$		—	
$\log_{10}(R_{\rm cut}^{\rm Gal}/{\rm V})$	17.48 ± 0.02		—	
EG components (at the escape)	LE	HE	LE	HE
$\mathcal{L}_0$ [$10^{44}\cdot \rm erg\cdot Mpc^{-3}\cdot yr^{-1}$] *	6.54 ± 0.36	5.00 ± 0.35	11.35 ± 0.15	5.07 ± 0.06
γ	3.34 ± 0.07	-1.47 ± 0.13	3.52 ± 0.03	-1.99 ± 0.11
$\log_{10}(R_{\rm cut}/{\rm V})$	> 19.3	18.19 ± 0.02	> 19.4	18.15 ± 0.01
$I_{\rm H}$ (%)	100 (fixed)	0.0 ± 0.0	48.7 ± 0.3	0.0 ± 0.0
$I_{\rm He}$ (%)	—	24.5 ± 3.0	7.3 ± 0.4	23.6 ± 1.6
$I_{\rm N}$ (%)	—	68.1 ± 5.0	44.0 ± 0.4	72.1 ± 3.3
$I_{\rm Si}$ (%)	—	4.9 ± 3.9	0.0 ± 0.0	1.3 ± 1.3
$I_{\rm Fe}$ (%)	—	2.5 ± 0.2	0.0 ± 0.0	3.1 ± 1.3
D_J (N_J)	48.6 (24)		56.6 (24)	
$D_{X_{\rm max}}$ ($N_{X_{\rm max}}$)	537.4 (329)		516.5 (329)	
D (N)	586.0 (353)		573.1 (353)	

* from $E_{\rm min} = 10^{17.8}$ eV.

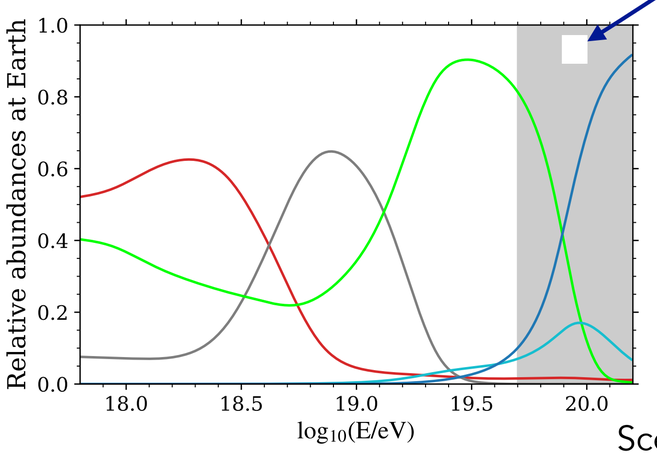

Energy spectrum at the Earth

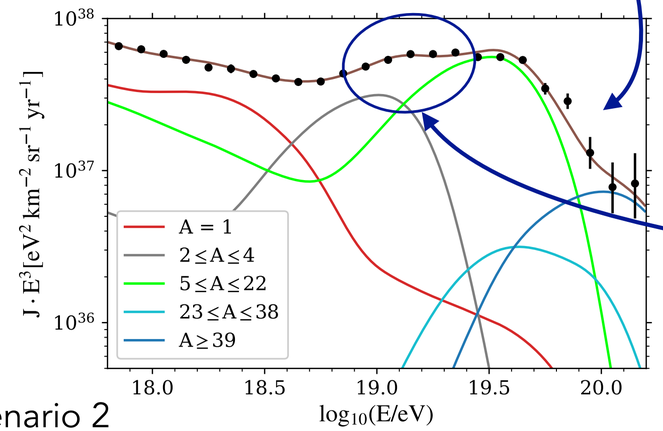

Scenario 2

New observed feature at 13 EeV

→ interplay between He and N components ejected at the sources according to their R-dependent cutoff and then shaped by propagation

Results in the reference scenarios

Some common findings between the two scenarios:

Very high rigidity cutoff of the LE component

- Degenerate fit for $R_{cut}^{LE} \gg 10^{19.5}$eV
  - → fixing the parameter to any much higher value does not change the fit
  - → only the lower bound
- The LE component is very steep
  - → dominant only in the first energy bins
  - → not very sensitive to the energy spectrum shape

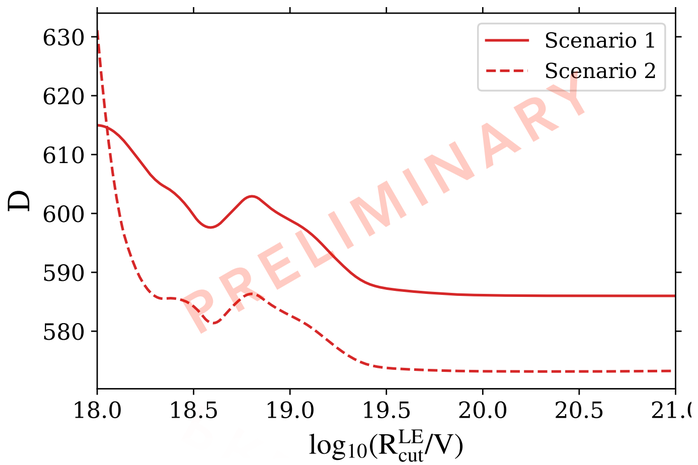

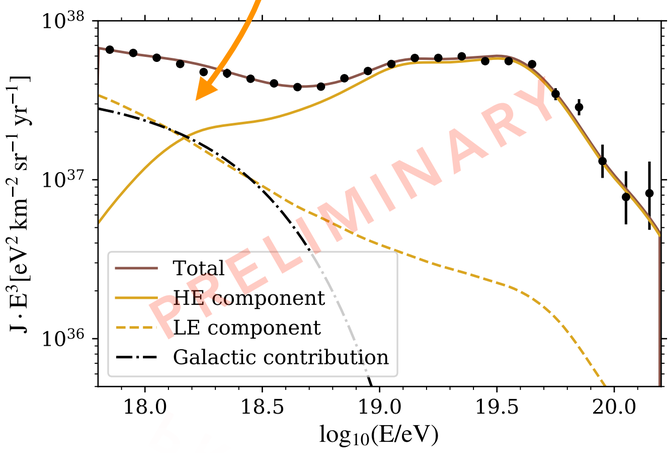

	Scenario 1		Scenario 2	
Galactic contribution (at Earth)	pure N		—	
$J_0^{\rm Gal}$ [eV$^{-1}\cdot$km$^{-2}\cdot$sr$^{-1}\cdot$yr^{-1}]	$(1.06 \pm 0.04)\cdot 10^{-13}$		—	
$\log_{10}(R_{\rm cut}^{\rm Gal}/{\rm V})$	17.48 ± 0.02		—	
EG components (at the escape)	LE	HE	LE	HE
$\mathcal{L}_0$ [$10^{44}\cdot$erg$\cdot$Mpc$^{-3}\cdot$yr^{-1}] *	6.54 ± 0.36	5.00 ± 0.35	11.35 ± 0.15	5.07 ± 0.06
γ	3.34 ± 0.07	-1.47 ± 0.13	3.52 ± 0.03	-1.99 ± 0.11
$\log_{10}(R_{\rm cut}/{\rm V})$	> 19.3	18.19 ± 0.02	> 19.4	18.15 ± 0.01
$I_{\rm H}$ (%)	100 (fixed)	0.0 ± 0.0	48.7 ± 0.3	0.0 ± 0.0
$I_{\rm He}$ (%)	—	24.5 ± 3.0	7.3 ± 0.4	23.6 ± 1.6
$I_{\rm N}$ (%)	—	68.1 ± 5.0	44.0 ± 0.4	72.1 ± 3.3
$I_{\rm Si}$ (%)	—	4.9 ± 3.9	0.0 ± 0.0	1.3 ± 1.3
$I_{\rm Fe}$ (%)	—	2.5 ± 0.2	0.0 ± 0.0	3.1 ± 1.3
D_J (N_J)	48.6 (24)		56.6 (24)	
$D_{X_{\rm max}}$ ($N_{X_{\rm max}}$)	537.4 (329)		516.5 (329)	
D (N)	586.0 (353)		573.1 (353)	

* from $E_{\rm min} = 10^{17.8}$ eV.

Results in the reference scenarios

The mass composition in the LE region

Mixture of H+N below the ankle in both scenarios

Galactic component in Scenario 1 :

- power law modified by an exponential cutoff with some free parameters
- Models with Galactic Fe/Si right below the ankle are strongly disfavored
- **a N-dominated composition is preferred**

  → contribution from explosions in the winds of Wolf-Rayet-like stars may provide N up to ~10^{18} eV

<u>It is not possible to choose a favored scenario</u>

- Scenario 2: better X_{max} distributions and worse spectrum description
- The **differences are encompassed within the systematic uncertainties**
- In Scenario 2, photodisintegration is negligible for the LE component

  → light-to-intermediate masses (similar to the one at the sources)
- Further investigation of the Galactic-to-extragalactic transition region is necessary

	Scenario 1		Scenario 2	
Galactic contribution (at Earth)	pure N		—	
$J_0^{\rm Gal}$ $[{\rm eV}^{-1}\cdot{\rm km}^{-2}\cdot{\rm sr}^{-1}\cdot{\rm yr}^{-1}]$	$(1.06\pm0.04)\cdot10^{-13}$		—	
$\log_{10}(R_{\rm cut}^{\rm Gal}/{\rm V})$	17.48 ± 0.02		—	
EG components (at the escape)	LE	HE	LE	HE
$\mathcal{L}_0$ $[10^{44}\cdot{\rm erg}\cdot{\rm Mpc}^{-3}\cdot{\rm yr}^{-1}]$ *	6.54 ± 0.36	5.00 ± 0.35	11.35 ± 0.15	5.07 ± 0.06
γ	3.34 ± 0.07	-1.47 ± 0.13	3.52 ± 0.03	-1.99 ± 0.11
$\log_{10}(R_{\rm cut}/{\rm V})$	>19.3	18.19 ± 0.02	>19.4	18.15 ± 0.01
$I_{\rm H}$ (%)	100 (fixed)	0.0 ± 0.0	48.7 ± 0.3	0.0 ± 0.0
$I_{\rm He}$ (%)	—	24.5 ± 3.0	7.3 ± 0.4	23.6 ± 1.6
$I_{\rm N}$ (%)	—	68.1 ± 5.0	44.0 ± 0.4	72.1 ± 3.3
$I_{\rm Si}$ (%)	—	4.9 ± 3.9	0.0 ± 0.0	1.3 ± 1.3
$I_{\rm Fe}$ (%)	—	2.5 ± 0.2	0.0 ± 0.0	3.1 ± 1.3
D_J (N_J)	48.6 (24)		56.6 (24)	
$D_{X_{\rm max}}$ $(N_{X_{\rm max}})$	537.4 (329)		516.5 (329)	
D (N)	586.0 (353)		573.1 (353)	

* from $E_{\rm min}=10^{17.8}$ eV.

Effect of the systematic uncertainties from measurements

The systematic uncertainty effect is tested in the Scenario 2

Two main sources of experimental systematic uncertainties:

- **Energy scale:** $\sigma_{\rm sys}(E)/E = 14\,\%$
- **X_{max} scale:** $\sigma_{\rm sys}(X_{\rm max}) = 6 \div 9\ {\rm g\ cm^{-2}}$

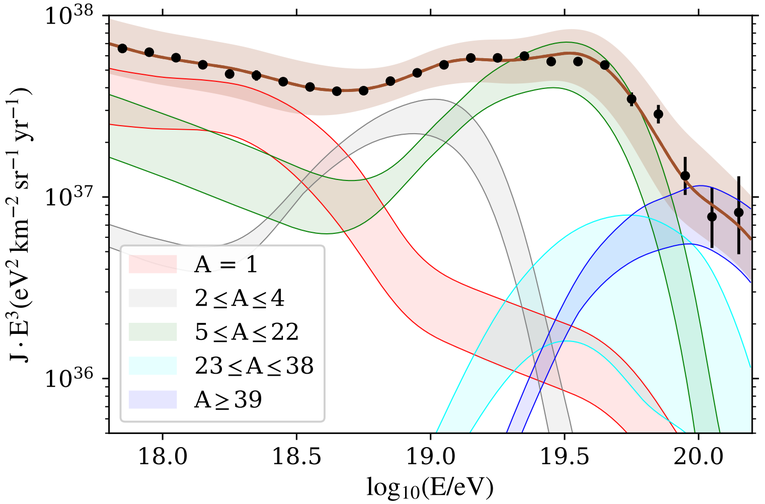

- Energy scale → shift all the energies of $\pm 1\sigma_E$ in each direction
- X_{max} scale → the correlations among the energy bins are taken into account allowing for different shifts at different energies
  - The X_{max} values are shifted by $a \cdot v_1(E) + b \cdot v_2(E)$
  - a, b are two additional nuisance parameters in the fit
  - A term $D_{syst} = a^2 + b^2$ has to be added to deviance

- ***Large band around the total flux*** due to the energy scale uncertainty → impact mainly on the estimated emissivity of sources
- The ***strongest impact*** on the predicted fluxes and on the deviance is due to the X_{max} scale uncertainty

Effect of the systematic uncertainties from models

Models for propagation in the IGM and in the atmosphere

σ_{pd}	**T**alys, **P**SB
EBL	**G**ilmore, **D**ominguez
HIM	**E**POS-LHC, **S**ibyll2.3d, **Q**GSJetIIv4

Hadronic interaction model: Sibyll2.3d / EPOS-LHC / intermediate models

- Nuisance parameter δ_{HIM} to interpolate each Gumbel parameter as $\alpha_{\mathrm{HIM}} = \delta_{\mathrm{HIM}} \cdot \alpha_{\mathrm{EPOS}} + (1 - \delta_{\mathrm{HIM}}) \cdot \alpha_{\mathrm{Sib}}$
- If δ_{HIM} is close to 0 → Sibyll2.3d is dominant
- If δ_{HIM} is close to 1 → EPOS-LHC is dominant

Propagation model effect:

fit repeated considering different model configurations

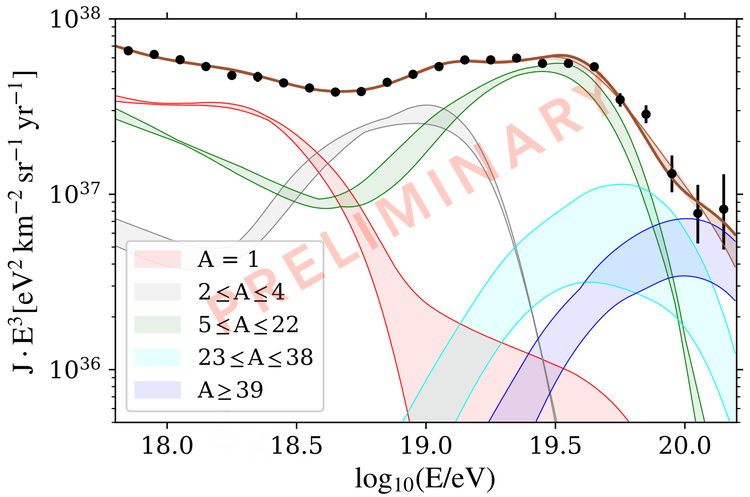

- *EPOS-LHC or models compatible with it are always preferred*
  → **HIM choice: stronger impact on D and on the predictions at Earth**
- *Propagation models*: some expected changes in the best fit parameters

The dominant effect on the the predicted fluxes and on the deviance is the one from the experimental uncertainties

Combined fit with arrival directions

- Combined fit approach above the ankle involving energy spectrum, shower maximum depth distributions and arrival directions (additional term in the log likelihood)
- **Contribution from SBG / γ-AGN catalogs or Cen A as a single source** is added to the one of the homogeneous background
- Different source evolutions are considered for the background (flat or positive with m=3,5)
- A test statistic measures the improvement given by the catalog

  → the Cen A model with flat evolution is the best fit

  → largest test statistic obtained with the SBG model
- **γ-AGN model is disfavoured by Auger data (negative test statistic) due to the strong contribution of the distant blazar Markarian 421**

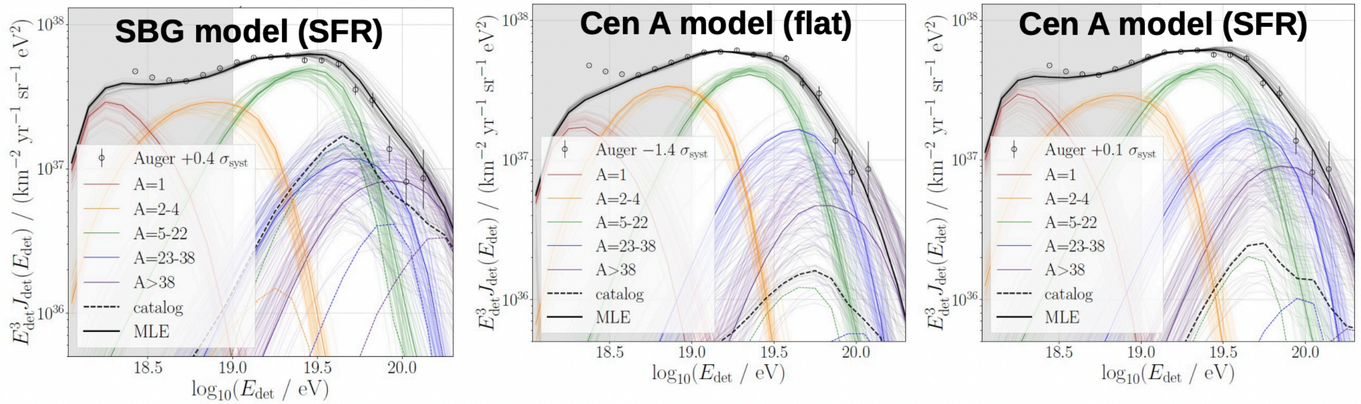

Intergalactic magnetic fields

Larmor radius: $r_{\rm L} \approx 1.08 \cdot (E/{\rm EeV}) \cdot Z^{-1} \cdot (B_\perp/{\rm nG})^{-1}\ {\rm Mpc}$

Propagation theorem: the effect of intergalactic magnetic fields is negligible if the distance among sources is much lower than $r_{\rm L}$

- The lowest relevant rigidity ~E/Z in our model is that of N (Z=7) at ~$10^{17.8}$ eV
- Typical distance among sources is $\lesssim 10\,{\rm Mpc}$

→ **magnetic fields should have $B_\perp \ll 10^{-11}$ G to be negligible**